Review

Ubiquinol oxidation in the cytochrome bc_1 complex: Reaction mechanism and prevention of short-circuiting

Armen Y. Mulkidjanian*

Max Planck Institute of Biophysics, Department of Biophysical Chemistry, Max-von-Laue-Str. 3, D-60438 Frankfurt-am-Main, Germany
Department of Biophysics, School of Biology and Chemistry, University of Osnabrück, D-49069 Osnabrück, Germany
A.N. Belozersky Institute of Physico-Chemical Biology, Moscow State University, 119899 Moscow, Russia

Abstract

This review is focused on the mechanism of ubiquinol oxidation by the cytochrome bc_1 complex (bc_1). This integral membrane complex serves as a "hub" in the vast majority of electron transfer chains. The bc_1 oxidizes a ubiquinol molecule to ubiquinone by a unique "bifurcated" reaction where the two released electrons go to different acceptors: one is accepted by the mobile redox active domain of the [2Fe-2S] iron–sulfur Rieske protein (FeS protein) and the other goes to cytochrome b. The nature of intermediates in this reaction remains unclear. It is also debatable how the enzyme prevents short-circuiting that could happen if both electrons escape to the FeS protein. Here, I consider a reaction mechanism that (i) agrees with the available experimental data, (ii) entails three traits preventing the short-circuiting in bc_1, and (iii) exploits the evident structural similarity of the ubiquinone binding sites in the bc_1 and the bacterial photosynthetic reaction center (RC). Based on the latter congruence, it is suggested that the reaction route of ubiquinol oxidation by bc_1 is a reversal of that leading to the ubiquinol formation in the RC. The rate-limiting step of ubiquinol oxidation is then the re-location of a ubiquinol molecule from its stand-by site within cytochrome b into a catalytic site, which is formed only transiently, after docking of the mobile redox domain of the FeS protein to cytochrome b. In the catalytic site, the quinone ring is stabilized by Glu-272 of cytochrome b and His-161 of the FeS protein. The short circuiting is prevented as long as: (i) the formed semiquinone anion remains bound to the reduced FeS domain and impedes its undocking, so that the second electron is forced to go to cytochrome b; (ii) even after ubiquinol is fully oxidized, the reduced FeS domain remains docked to cytochrome b until electron(s) pass through cytochrome b; (iii) if cytochrome b becomes (over)reduced, the binding and oxidation of further ubiquinol molecules is hampered; the reason is that the Glu-272 residue is turned towards the reduced hemes of cytochrome b and is protonated to stabilize the surplus negative charge; in this state, this residue cannot participate in the binding/stabilization of a ubiquinol molecule.
© 2005 Elsevier B.V. All rights reserved.

1. Introduction

Cytochrome bc_1-complexes of animals and bacteria (hereafter bc_1), as well as closely related cytochrome b_6f-complexes of plants and cyanobacteria (hereafter bf), are oligomeric membrane enzymes that function as electrogenic quinol:cytochrome c oxidoreductases (see [1,2] for comprehensive reviews on bc_1 and bf, respectively). These membrane complexes catalyze the oxidation of diverse quinols by high potential redox-carriers (c-type cytochromes in mitochondria and bacteria or plastocyanin in cyanobacteria and higher plants). The free energy of the redox reaction is used to transfer protons across the energy-transducing membrane. Thereby, one of the membrane-adjoining water phases becomes positively charged (p-side) whereas the other one charges negatively (n-side). Proton transfer leads to the formation of the difference in electrochemical activity of

* Abteilung Biophysik, Fachbereich Biologie/Chemie, Universität Osnabrück, D-49069 Osnabrück, Germany. Tel.: +49 541 9692871; fax: +49 541 9692870.

E-mail address: mulkidjanian@biologie.uni-osnabrueck.de.

protons across the membrane ($\Delta\mu_{H+}$). The latter can be considered as a sum of chemical (ΔpH) and electrical ($\Delta\psi$) components and reaches approximately 200–250 mV under physiological conditions [3]. Thus, bc_1 has to pump protons against remarkable backpressure at steady state.

The cytochrome bc_1 complex (see Fig. 1) is an intertwined dimer both in crystals [4–11] and in solution [12]. The catalytic core of each bc_1 monomer is formed by three subunits: the membrane-embedded cytochrome b, the [2Fe–2S] cluster-carrying Rieske protein, and cytochrome c_1 (see Fig. 1). Each cytochrome b carries one low- and one high-potential protoheme (b_1 and b_h, respectively, the redox and spectroscopic properties of the cofactors are given in Table 1). The number of subunits in cytochrome bc-complexes varies from only 3 catalytic ones in some bacteria up to 11 in the mitochondrial bc_1.

With bc_1-containing proteoliposomes, it was shown that two protons were transferred across the membrane per each oxidized quinol [13,14]. Mitchell has explained this stoichiometry by a Q-cycle mechanism [15,16]. The mechanism invoked the bifurcation of electron flow at the site of quinol oxidation, as originally suggested by Wikström and Berden [17], with one electron reducing cytochromes c and another one going to cytochrome b. In addition, Q-cycle implied that electrons, after passing through cytochrome b, reduce a quinone molecule from the other side of the membrane as shown in Fig. 1. According to the current, structure-based Q-cycle models (see e.g., [1,6,8,18–20]), quinol molecules are oxidized at the interface between cytochrome b and the mobile [2Fe–2S] cluster-carrying domain of the Rieske protein (hereafter the FeS domain, see Fig. 1). This interface forms the

catalytic center P of the enzyme (which corresponds to center o in the original Mitchell's notation). The FeS domain takes the first electron from a ubiquinol to pass it further, via cytochrome c_1 and the further c-type cytochromes (cytochrome c in mitochondria and cytochromes c_y and c_2 in phototrophic bacteria [21]), to external electron carriers. The semiquinone remaining in center P reduces the heme b_l. From this heme, the electron moves across the membrane to heme b_h and then to the further quinone-binding center N (center i in the Mitchell's notation). In center N, a ubiquinone molecule is reduced first to a semiquinone anion $Q_N^{\bullet-}$ and then, after the oxidation of the next ubiquinol in center P, to a Q_NH_2 ubiquinol. This ubiquinol can be oxidized by bc_1 as well, so that two charges are "pumped" across the membrane per each ubiquinol processed by bc_1. It is convenient to distinguish two electron transfer (ET) branches in bc_1, namely the high-potential one, which is formed by the FeS domain and cytochrome c_1 (c-chain according to [20]), and the low-potential one formed by two hemes of cytochrome b and the Q_N quinone (b-chain).

The Mitchell's idea of doubling the enzyme efficiency by the internal electron cycling is generally accepted (see, however, [22]). Further details on the enzyme reaction remain still controversial. It is debatable whether ubiquinol is oxidized sequentially, in two steps, or this reaction is concerted. There are diverse hypotheses explaining why both electrons, which are released upon quinol oxidation, do not escape via the FeS domain towards cytochromes c.

In this review, the ubiquinol oxidation in center P of bc_1 is compared with the reduction of the secondary quinone Q_B in the photosynthetic reaction center (RC) of purple photo-
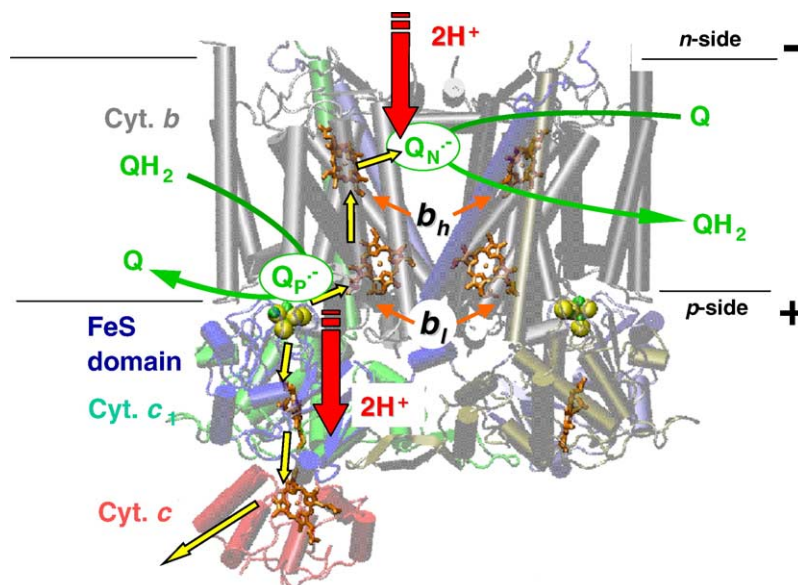

Fig. 1. Overview of structure and function of the cytochrome bc_1 complex. The scheme shows the Q-cycle scheme superimposed on the X-ray structure of the three catalytic subunits of the dimeric yeast bc_1. The X-ray structure of the yeast bc_1 co-crystallized with cytochrome c (PDB entry 1KYO [10]) was used for the presentation. Color code: grey/black, cytochrome b subunits; blue, thick line, the Rieske subunits; green, cytochromes c_1; red, cytochrome c; yellow, hemes. Figure was produced with the help of the VMD software package [216].

Table 1
Cytochrome bc_1 complex of *Rb. capsulatus*: electrochemical and spectral properties of the redox cofactors

Redox cofactor	E_m^7 (mV)	λ_{max} (nm)	g_x (EPR)
Heme b_1	−90/−115 mV (heme b_h reduced)[a,b] approximately 0 mV (heme b_h oxidized)[c,d]	558/565[a,b]	
Heme b_h	+50/+60 mV[a,b]	560,5[a,b]	
cytochrome c_1	+290/+340 mV[e,f]	552[e]	
[2Fe−2S] cluster	+270 (FeS$_c$)[a,g]/+460 mV (FeS$_b$)[h]	−	1.800 (ubiquinone present)[i] 1.774 (ubiquinone absent)[i]

References: a, [213]; b, [33]; c, [214]; d, [64]; e, [56]; f, [215]; g, [106]; h, [109]; i, [45].

synthetic bacteria. The mechanism of the latter reaction is well understood because it is possible to feed electrons into the RC one by one by firing short flashes of light, so that intermediate states can be trapped and studied (see e.g., [23–29]). So far, the parallels were drawn between the mechanisms of sequential ubiquinone *reduction* in the RC and in the center N of bc_1 [9,19,30–32]. As argued below, the quinone-processing machinery in the RC can serve as useful paradigm for understanding the mechanism of the bifurcated ubiquinol *oxidation* by bc_1 as well.

2. Mechanism of ubiquinol oxidation by the cytochrome bc_1 complex

2.1. Electron cycling in chromatophore vesicles from purple phototrophic bacteria

The data on the operation of bc_1 in a flash-triggered mode, as discussed in the following sections, were mostly obtained with preparations of chromatophores (inside-out vesicles of inner cellular membrane) from purple photo-trophic bacteria *Rhodobacter sphaeroides* and *Rhodobacter capsulatus* (see Fig. 2 and [33–35] for reviews).

Absorption of light quantum by photosynthetic pigments leads to the electrogenic transmembrane charge separation in the photosynthetic reaction center (RC, see Fig. 3) and to generation of a reducing agent (Q_BH_2 ubiquinol) and of an oxidant (oxidized cytochrome c_2) for bc_1. The cytochrome bc_1 complex catalyzes the ET from ubiquinol back to cytochrome c_2 (see Fig. 2); this reaction is coupled with $\Delta\psi$ generation (see [3,33,34] for reviews). The flash-induced redox changes of cytochromes can be monitored optically [36,37], whereas the generation of $\Delta\psi$ can be followed both optically, via the electrochromic shifts of intramembrane carotenoids [38,39], and by capacitive electrometry [39,40]. The reactions of proton binding and release could be traced by appropriate pH-indicators [41–43]. The reactions in bc_1 are routinely discriminated by application of inhibitors that selectively block quinol
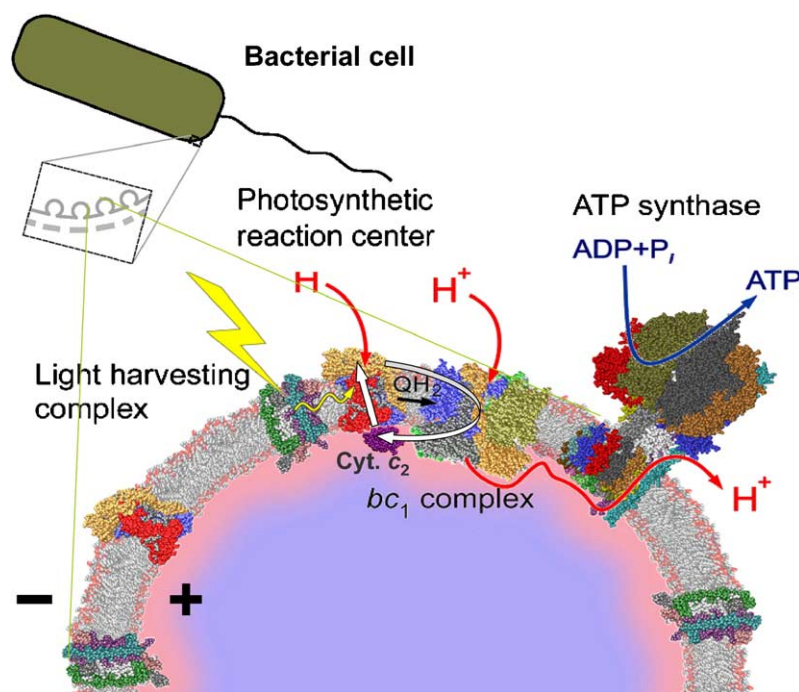

Fig. 2. Schematic presentation of a chromatophore membrane based on a picture by Boris Feniouk. White arrows depict electron cycling between the RC and the bc_1. The red color of the interfacial water layer indicates its higher acidity at steady state, which can increase the protonic backpressure on the cytochrome bc_1 complex [217,218].
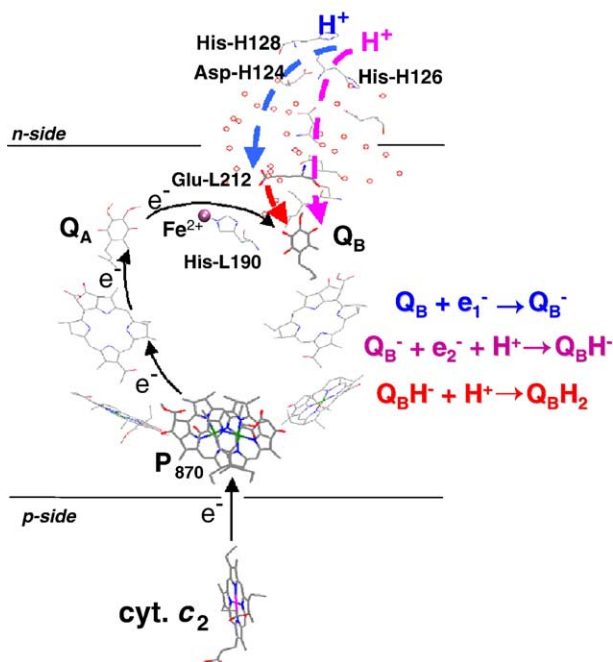
Fig. 3. Schematic presentation of electron and proton transfer events in the RC of *Rb. sphaeroides*. The scheme is a compilation of the RC structure with a Q_B in the proximal (catalytic) position (PDB entry 1PCR [219]) and of the (Q_B-depleted) X-ray structure of the RC co-crystallized with cytochrome c_2 (PDB entry 1L9B [220]). After the charge separation, electron goes from the primary electron donor P_{870} first to the primary electron acceptor Q_A and then to the secondary quinone acceptor Q_B, which is reduced and protonated in two steps. The neutral forms of the latter are mobile, so that the formed ubiquinol can leave the RC to be eventually oxidized by bc_1. The route of proton transfer from the water phase to Q_B, via the Zn^{2+}-binding site formed by Asp-H124, His-H126, and His-H128 of the H-subunit, is reconstructed based on the data of Paddock et al. (see [28] and references cited therein). Element color code: oxygen, red; nitrogen, blue; iron, violet; magnesium, green. The color of proton transfer steps corresponds to the color of the respective partial reactions as depicted on the picture.

oxidation (e.g., of myxothiazol) and by comparison of the kinetic traces in the presence and in the absence of an inhibitor.

Besides providing the possibility to study the bc_1 in a pulsed mode, chromatophores have several other advantages: (i) the bc_1 complexes of purple bacteria are simple and are made of only 3 or 4 subunits [11,35,44,45]; (ii) chromatophore vesicles are easy to isolate; they remain stable at room temperature for many hours; (iii) mutants with site-specific amino acid substitutions in the subunits of the bc_1 are available (see [46] for their survey); (iv) evolutionarily, purple bacteria are close to mitochondria [47]; not surprisingly, the X-ray structure of the simplest three-subunit bc_1 from *Rb. capsulatus*, which has been recently resolved up to 3.8 Å [11], overlaps with the three core subunits of the mitochondrial bc_1, and the same specific inhibitors are effective in both systems.

When the membrane quinones are oxidized in the dark, the flash-induced turnover of bc_1 is triggered by the arrival of a ubiquinol molecule formed in the RC. At neutral pH, the

oxidation of this ubiquinol by bc_1 leads to a partial reduction of heme b_h at approximately 3 ms followed by slower (i) re-reduction of the flash-oxidized cytochrome c_1 by electrons coming from ubiquinol, (ii) $\Delta\psi$ generation, and (iii) proton release to the p-side of the membrane. These three reactions take approximately 10–20 ms [18,36,39,43,48–51]. Usually, there are 2–3 RCs per one bc_1 monomer in the membranes of *Rhodobacter*, so that each bc_1 dimer turns over several times after a saturating flash of light. Therefore, the kinetic mismatch between the faster heme b_h reduction and slower cytochrome c_1 re-reduction and electrogenesis was usually explained by the contribution of the multiple turnovers of bc_1 to the latter reactions (see e.g., [52]). The cytochrome bc_1 complex can be, however, compelled to turn over only once (i) if the substrate ubiquinol is in shortage [18,53] or (ii) if the exciting flash is weak [51,54]. Under such conditions, the heme b_h was still reduced at 3 ms, whereas the flash-induced $\Delta\psi$ generation and cytochrome c re-reduction proceeded at approximately 30–40 ms, by order of magnitude slower [18,51,53].

Under reducing conditions, when ubiquinol is abundant in the membrane (that corresponds to the native situation [55]), the oxidation of ubiquinol by bc_1 is triggered by the migration of an electron vacancy, via cytochromes c, to the FeS domain ([56], see Fig. 1). In flash experiments, the ubiquinol oxidation by bc_1 manifests itself in the re-reduction of cytochromes c at 2–4 ms. The kinetics of this re-reduction corresponds to the kinetics of $\Delta\psi$ generation by bc_1. No flash-induced redox changes of cytochrome b can be resolved: apparently, under these conditions, the latter is oxidized faster than is reduced (for reviews, see [33,34,36]).

Recently, it has been found that the implementation of Zn^{2+}, a well-established inhibitor of the mitochondrial bc_1 [57,58], can help to resolve the partial reactions in an intact bc_1 even under reducing conditions [54,59]. The Zn^{2+} ions retarded the oxidation of heme b_h and made the kinetics of its reduction visible. In the presence of <100 µM Zn^{2+}, the electrogenic reaction in bc_1 slowed down but retained its full extent. The latter observation indicated that the bc_1 complexes remained fully functional. The flash-induced oxidation of ubiquinol led to the reduction of heme b_h at 1.5–2 ms. The re-reduction of cytochrome c_1 by ubiquinol, the $\Delta\psi$ generation, and the proton release into the chromatophore interior took about 10 ms. The retardation of the latter reactions relative to the heme b_h reduction was apparent even after a weak flash of light, which triggered only one turnover in some bc_1 monomers [54,59].

One conclusion from these data was that the turnover of bc_1 proceeds in two steps, at least, as depicted in Fig. 4 (see also [54,59]). During the first, faster step (see Fig. 4A), a ubiquinol molecule is oxidized in center P, and two electrons arrive at the FeS cluster and at heme b_h, respectively. During the second, slower step protons are released from center P, $\Delta\psi$ is generated, and cytochrome c_1
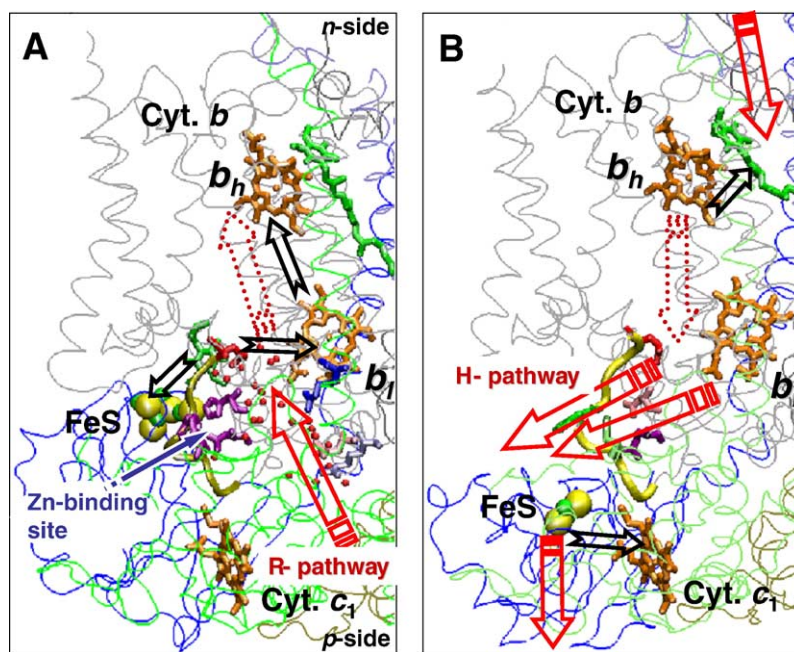
Fig. 4. Tentative scheme of electron and proton transfer during the initial steps of bc_1 turnover (modified from Fig. 2 in [59]). Black arrows, ET events; red arrows, proton transfer events; dark red dotted arrows, dielectric relaxation of protein/water. The redox centers are colored as in Fig. 1. The Glu-272 of cytochrome b is colored red. The segment of the ef loop that interferes with the movement of the FeS domain (cytochrome b residues from 260 to 270, avian numeration) is shown as a thick yellow tube. (A) Fast step of ubiquinol oxidation in center P. The picture is a compilation of two crystal structures of the yeast bc_1: the water chains from the high resolution structure (PDB entry 1EZV [9]) are superimposed over the structure of a dimeric yeast bc_1 co-crystallized with cytochrome c (PDB entry 1KYO [10]). The bound stigmatellin in center P was replaced by ubiquinone. Water molecules, which are found in the vicinity of center P are shown as red balls. The four amino acid residues, which correspond to the Zn^{2+}-binding ligands of the chicken bc_1, are depicted in violet (thereby Ser-268 of yeast was replaced by histidine, as in *Rb. capsulatus* and chicken; other residues are His-253, Asp-255 of cytochrome b and His-185 of cytochrome c_1). The charged residues of cytochrome b involved in the R-pathway are colored as following: Arg-79, dark blue; Arg-70, light blue; and Asp-71, pink. (B) Slower step of ubiquinone reduction in center N. The picture is based on the structure of the chicken bc_1 (PDB entry 1BCC [6]). Ubiquinol in center N is shown in the same position as it is found in the yeast bc_1 (PDB entry 1KYO [10]). The four amino acid residues, which bind Zn^{2+} in the chicken bc_1 are colored as follows: Asp-253, pink; Glu-255, violet; His-268, green (all three are residues of cytochrome b); His-121 of cytochrome c_1, light green.

is re-reduced by the FeS cluster, as depicted in Fig. 4B. These slower reactions seem to correlate with the oxidation of heme b_h in center N. In this review, we focus on the first, faster step of ubiquinol oxidation. The slower events are considered only in relation to the prevention of short circuits in bc_1 (see Sections 2.5.1 and 3.2).

Another conclusion from the data was that the flash-induced reduction of heme b_h was not accompanied by a compatibly fast $\Delta\psi$ generation in an intact bc_1 [54,59]. Hence, the transmembrane ET from center P to heme b_h over a distance of >20 Å (see Fig. 4) was electrically compensated. This situation differs from that in the RC where the transmembrane charge separation is accompanied by pronounced electrogenesis [38]. Seemingly paradoxical, the electrical silence of the transmembrane ET towards heme b_h could be due to the small driving force of the reaction. As it has been argued elsewhere, the low-exothermic ET reactions in proteins can be controlled/driven by the medium relaxation [60,61]. In other words, if the reaction driving force $|\Delta G|$ is small, the initial electron exchange between reactants brings the system into an intermediate, unrelaxed state, the energy level of which might lie *above* that of the initial state (see Fig. 5 and its legend). In this case, the *observable* ET is driven by the

relaxation of this intermediate state into the final one (red arrow in Fig. 5A and the transition between the solid and dashed blue energy terms in Fig. 5B). In other words, the *observable* ET follows the protein relaxation around the redox center(s). As shown by Dutton et al., the rate constant of ET in proteins depends on the edge-to-edge distance between reactants R as $\log_{10} k = 15 - 0.6R - 3.1(\Delta G + \lambda)^2/\lambda$ where λ is the medium reorganization energy [62]. If the ET rate is by orders of magnitude slower than expected from this empirical relation, a relaxation control over ET might be the reason. As it is argued in refs. [60,61], the observable rate of biological ET is likely to be determined by the rate of protein reorganization if $|\Delta G| < 100$ meV.

While the transmembrane charge separation in the RC is a highly exothermic reaction with ΔG of <-400 meV (see e.g., [36]), the driving force for heme b_h reduction by heme b_l is much smaller. The equilibrium constant of the $b_l \leftrightarrow b_h$ reaction has been shown to be 10–15 at pH 7 [63], which corresponds to a ΔG value of electron transfer between b_l and b_h of about $-60/-100$ meV at equilibrium and in the *absence* of $\Delta\psi$. In the *presence* of $\Delta\psi$, which counteracts the ET from heme b_l to heme b_h, the respective ΔG value is likely to approach zero, so that electrons can
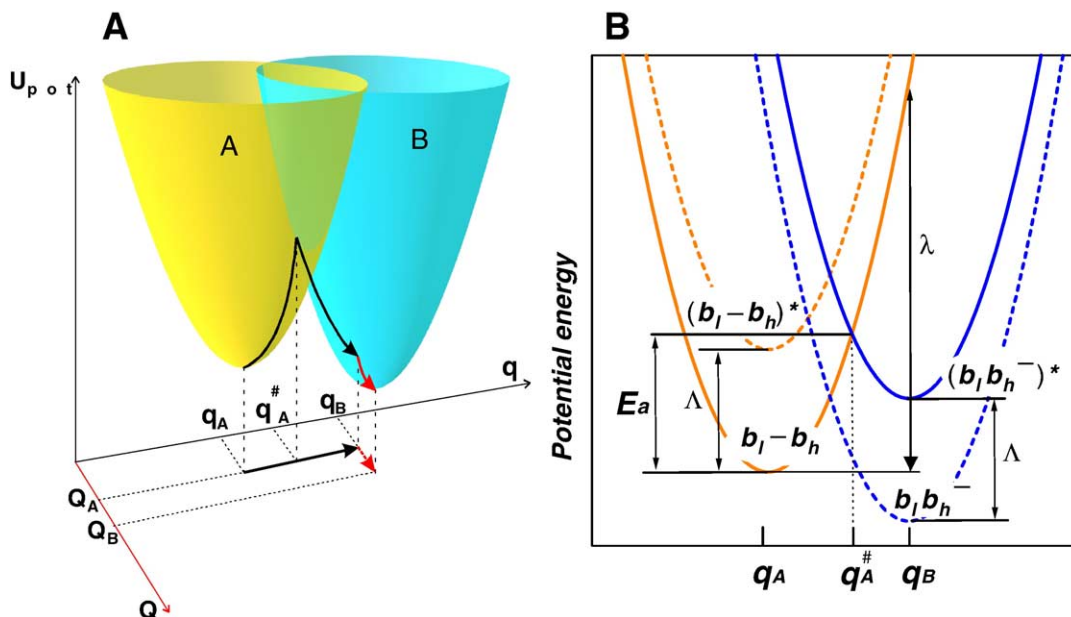
Fig. 5. Scheme of relaxationally controlled ET (modified from Fig. 1 in [61]). The fast non-adiabatic ET in the system is visualized by the reaction coordinate q, whereas the slower medium reorganization proceeds along the coordinate Q. The potential energy in the precursor electronic state A is shown by the left yellow paraboloid in A and by the left orange parabolic curves in B. The product state B corresponds to the right blue paraboloid in A and to the right blue parabolas in B. (A) Three-dimensional diagram. In the precursor state, the reactants are thermally equilibrated in the potential well A on the left. The transition of the precursor state into the product one occurs at the intersection of two paraboloids. Due to the fast thermal motion along the coordinate q, the system reaches the transient configuration ($q_A^{\#}$,Q_A) at constant value of coordinate Q (upward arrow). The following fast relaxation of the system along the coordinate q (downward arrow) stabilizes the product state B only partially. The complete stabilization requires the rearrangement of the system along the slow coordinate Q (red arrow). (B) Two-dimensional cross-section of the energy diagram in A as adapted for the case of ET between heme b_1 and heme b_h in bc_1. The parabolic potential energy profiles of the precursor (orange, left) and product (blue, right) electronic states are shown at two values of the relaxation coordinate Q: the solid curves are plotted at Q = Q_A, the dashed curves are plotted at Q = Q_B, respectively. Here the unrelaxed intermediate state of bc_1 with heme b_h reduced ($b_1b_h^-$)* corresponds to the solid blue energy term, whereas the relaxed final state $b_1b_h^-$ is depicted by a dashed blue curve (see Section 2.1 and [61] for further details).

flow from heme b_1 to heme b_h only on condition of electrical compensation. In this case, however, the ET from b_1 to b_h would not be accompanied by notable $\Delta\psi$ generation, in agreement with experimental observations [18,43,50,54,59,64]. Quite recently, by using ultra-fast microfluidic mixer and freeze-quenching device, coupled with EPR, Zhu et al. succeeded to determine the pre-steady state kinetic of ubiquinol oxidation by bc_1 [65]. The heme b_1 was reduced at 250 μs, simultaneously with the FeS cluster. The heme b_1 was reduced slower, at 2.5 ms (cf. with the above considered Zn^{2+}-treated chromatophores of *Rb. capsulatus* [54,59]). The Dutton's ruler [62] predicts, however, that the ET from heme b_1 to heme b_h, across the edge-to-edge distance of ∼10 Å, has to proceed at <1 μs, i.e., by three orders of magnitude faster than was actually observed [65]. Apparently, the reduction of heme b_h cannot proceed to completion unless compensated by protein.

The electrical compensation of the transmembrane ET could be due to the displacement of protons and/or charged protein groups. Notably, the E_m value of heme b_1 in *Rb. sphaeroides* is pH dependent in the whole physiological pH range [66,67], so that at neutral pH the reduction of heme b_1 is likely to be accompanied by protonation event(s). A water

chain connecting the propionates of heme b_1 with the water phase from the p-side of the membrane was predicted from molecular dynamics simulations [68] and found in the high-resolution X-ray structure of the yeast bc_1 [9]. This chain has been already suggested to participate in the electrostatic compensation of heme b_1 reduction [9]. Proton transfer towards the propionate groups of heme b_1 in response to its reduction, as shown in Fig. 4A, would contribute to the electrical silencing of the ET from heme b_1 to heme b_h because the rate-limiting step of ubiquinol oxidation is coupled with the preceding events in center P, not with the ET from heme b_1 to heme b_h proper (see [69] and Section 2.5.2). Another thinkable possibility is that the docking of the mobile FeS domain to cytochrome b, kinetically coupled with the reduction of heme b_h (see Section 2.5 below), might play a part in the electrical compensation of the ET across cytochrome b.

The dielectric relaxation can be also accomplished by dipole reorientation of water molecules, as shown schematically by dotted arrow in Fig. 4A. In the case of *Rps. viridis* RC, it has been shown that water molecules occupy the Q_B-binding cavity in the absence of the quinone molecule [70]. The same must be true for bc_1: water molecules are expected to penetrate the enzyme upon the

quinone retreat/exchange reactions in the four catalytic centers. Although mostly unresolvable in crystal structures, these water molecules still manifest themselves indirectly (see e.g., [71]).

Importantly, a reversion of those reactions that "silence" the electron on its way across the membrane would cause $\Delta\psi$ generation. Such a reversion is expected after the neutralization of the negative charge(s) at cytochrome b upon the reduction and protonation of a ubiquinone molecule in center N [43]. In the Zn^{2+}-treated bc_1 of $Rb.$ $capsulatus$, the $\Delta\psi$ generation indeed correlated with the oxidation of heme b_h [54,59]. The slowing of $\Delta\psi$ generation and of proton release by Zn^{2+} ions can be explained by a suggestion that the Histidine-rich Zn^{2+}-binding patch, as identified in the crystals of mitochondrial bc_1 [71], serves as a proton outlet from center P (H-pathway in Fig. 4B). Structurally, the patch resembles the proton inlet of the $Rb.$ $sphaeroides$ RC, which can be blocked by Zn^{2+} (see [28], Fig. 3, and Section 2.4). The involvement of the water chain leading to heme b_1 in proton release, as suggested by Crofts et al. [72], is less likely. This chain (R-pathway in Fig. 4A) is flanked by two strictly conserved aRginine residues, which are expected to hamper the proton release via this way. More likely is the involvement of this water chain in the electrostatic compensation of negative charge at heme b_1, as shown in Fig. 4A and discussed above (see also Sections 2.5.1 and 3.2 and refs. [54,59] for further details).

Because the flash-induced redox reactions of cytochrome b are hardly resolvable, many studies of bc_1 were done in the presence of antimycin A (hereafter antimycin, see [1,73] for reviews). Antimycin binds close to center N [8,31], blocks the oxidation of heme b_h and allows only a "half-turnover" of the enzyme. In chromatophores from $Rb.$ $sphaeroides$ and $Rb.$ $capsulatus$, the $\Delta\psi$ generation and proton release accelerate after the addition of antimycin, but dramatically diminish in magnitude. Thereby, these reactions become as fast as the reduction of heme b_h (see e.g., [18,39,51,65,74–76]). The fact that only one ubiquinol molecule is oxidized in the presence of antimycin cannot alone account for the similarity in kinetics. As noted above, under single-turnover conditions created by ubiquinol shortage or weak flashes (in the absence of antimycin!), the kinetic discrepancy between the faster heme b_h reduction, from one hand, and the slower cytochrome c_1 re-reduction, $\Delta\psi$ generation and proton release, from the other hand, was still observed. With the ubiquinone pool pre-oxidized, it even became more pronounced under single-turnover conditions. Under the latter conditions, the addition of antimycin accelerated the rate of $\Delta\psi$ generation by factor of 10, making it compatible with that of heme b_h reduction [18,51,53]. These observations indicate that in the untreated, intact bc_1 a single catalytic turnover proceeds differently than in the presence of antimycin. As argued elsewhere [51,54,59,77], antimycin seems to disrupt a conformational connection between centers N and P that couples the electrogenic proton release from center P with the reduction and protonation of Q_N (see also Sections 2.5.1 and 3.2).

2.2. Inhibitor-binding sites in the center P of the cytochrome bc_1 complex

Brandt, von Jagow, and their co-workers have identified two different inhibitor-binding sites in center P, one for stigmatellin and 3-n-undecyl-2-hydroxynaphthoquinone (UHDBT), and another one for the methoxy-acrylate-stylbene (MOA) and myxothiazol [78,79]. The X-ray structures of mitochondrial bc_1 confirmed the existence of two distinct, although partly overlapping inhibitor-binding sites at the junction of the $cd1$, $cd2$, and ef helical loops connecting the transmembrane helices of cytochrome b from the p-side of the membrane [5–9,31,80–83]. One of these sites is $proximal$ to heme b_1 and binds myxothiazol, MOA-type inhibitors, and a non-oxidizable ubiquinol analogue 2,3,4-trimethoxy-5-decyl-6-methyl-phenol (TMDMP) (see e.g., [81,83]). In the recent study of Esser et al. [83], three highly conserved residues from the $cd1$ helix, Gly142, Val145, and Ile146 (in bovine numeration) were identified as the critical ones for the inhibitor binding in this site. Another inhibitor binding site (the $distal$ one relative to heme b_1) is on the interface of cytochrome b and the FeS domain; it binds stigmatellin, UHDBT-type inhibitors, and famaxadone [6,8,9,81–84]. Esser et al. identified a strong involvement of the conserved PEWY motif of the ef loop as the main feature of inhibitor binding in this position [83].

Depending on the presence of inhibitors and crystallization conditions, the FeS domain was found in different positions, indicating its rotation by approximately $60°$ [5–9,31,82,83]. Stigmatellin, UHDBT, 2-nonyl-4-hydroxyquinoline N-oxide (NQNO), and famaxadon trapped the FeS domain closer to cytochrome b, as shown in Fig. 4A, whereas in the absence of these inhibitors or in the presence of myxothiazol the domain was found closer to cytochrome c_1, as depicted in Fig. 4B (see [1,32,83] for surveys). It was concluded that the FeS domain moves, upon shuttling an electron from center P to cytochrome c_1, from a position where the FeS cluster is close to b_1 (FeS$_b$ state) into the "cytochrome c_1" position, where the cluster interacts with the cytochrome c_1 heme (FeS$_c$ state) [5–9]. In addition, Iwata et al. have identified an intermediate, "loose" state of the FeS domain, halfway between these two positions [7]. Esser et al. have exploit the correlation between the position of the FeS domain and nature of inhibitor bound to classify the inhibitors of center P into two groups [83]. According to this classification, the subgroup Pm (mobile FeS domain) includes myxothiazol, MOA-type inhibitors, and azoxystrobulin, while stigmatellin, famaxadon, and UHDBT-type inhibitors form to the subgroup Pf (for fixed FeS domain).

2.3. Divergence of electron flows in the cytochrome bc_1 complex

The divergent pattern of inhibitor binding in center P and the mobility of the FeS domain are related to the divergence of electron fluxes in the bc_1. As noted in Introduction, it remains debatable why both electrons released at ubiquinol oxidation do not escape via the FeS cluster. The latter, just by turning over twice, could carry both electrons from ubiquinol to cytochromes c. The FeS cluster with its midpoint potential at pH 7.0 (E_m^7) of ≥ 300 mV seems to be a more attractive oxidant for the semiquinone in center P than the hemes of cytochrome b (see Table 1 for the E_m values). The electron bifurcation in center P is rather rigorous: when, in the presence of antimycin, both hemes of cytochrome b become reduced, the turnover rate of bc_1 drops to about 2% of its usual value although both the FeS cluster and cytochrome c_1, fully oxidized under these conditions, are ready to accept electrons from ubiquinol [73]. And the other way around, both hemes of cytochrome b, after being pre-reduced by light flashes in chromatophore vesicles from *Rhodobacter* treated by antimycin, stay reduced on a time scale of seconds [85], although a two-electron reduction of a quinone in center P seems to be thermodynamically favorable. The latter phenomenon is especially striking in the view of general reversibility of bc_1: a quinone in center P can be reduced by electrons coming via the FeS cluster in the presence of external membrane potential (see [86] and references cited therein). A potential danger of short-circuiting in bc_1 has been recently addressed by several authors [20,87,88].

Based on the dependence of inhibitor binding in center P on the redox state of bc_1, Brandt and von Jagow have advanced the general principle of a redox-dependent conformational switch to rationalize the obligatory electron bifurcation in bc_1 [78,79]. The tentative mechanisms of such a switch, as suggested so far, can be subdivided into two major groups. In one set of models, the escape of the second electron into the high-potential branch is prevented by the prompt dissociation of the reactants. It has been suggested that the FeS domain, initially docked to cytochrome b, promptly moves into the FeS$_c$ position close to cytochrome c_1 after being reduced [89,90]. It has been hypothesized that the oxidized FeS domain cannot dock back unless the heme b_l is oxidized [89]. In addition to the fast dissociation of the FeS domain from cytochrome b, the possibility of a semiquinone relocation into the alternative quinone-binding site close to heme b_l has been invoked to explain how the oxidation of semiquinone by the returning oxidized FeS domain is prevented [8,32,69]. This set of models, however, was essentially weakened by the finding that one ubiquinol molecule could be still oxidized in a bifurcated mode in chromatophores of *Rb. capsulatus* where the FeS$_b \rightarrow$ FeS$_c$ motion was blocked by a mutation [91].

Alternatively, the first electron can get transiently trapped at the FeS cluster. Then, the cluster cannot be reduced anymore, and the second electron is compelled to reduce heme b_l [8,18,32,51,54,59,92,93]. Initially, this type of mechanism was invoked to explain the faster reduction of heme b_h as compared to the re-reduction of cytochrome c_1 [51]. Thereby, it was hypothesized that the formation of a semiquinone in center P is coupled with the transition of the center into a "closed" conformation with the E_m value of the FeS cluster becoming (transiently) higher than the E_m value of cytochrome c_1 [51]. In this state, the FeS domain cannot promptly reduce cytochrome c_1. The hypothesis was based on the observation that the tightly binding stigmatellin, believed to be a semiquinone analogue, increased the E_m^7 value of the FeS cluster up to 540 mV in the mitochondrial bc_1 [94]. The "opening" of center P, leading to the decrease in the E_m value of FeS and to the transfer of the "trapped" electron to cytochrome c_1, was suggested to happen only after the oxidation of heme b_h in center N [51]. A semiquinone, which is bound to the FeS-cluster with an elevated E_m, was the key element also in the hypothetical model of Link, who, however, assumed that the high-potential state of the FeS cluster persists only until heme b_l is reduced by the semiquinone [92]. The mobility of the FeS-cluster could be incorporated in the tentative mechanisms of this type by a suggestion that the oxidation of the FeS cluster by cytochrome c_1 is prevented by the transient "locking" of the reduced FeS cluster in the cytochrome b position, as shown in Fig. 4A, too far away from cytochrome c_1 [8,18,32,54].[1] Kim et al. considered the possibility that the undocking of the FeS domain happens after the oxidation of heme b_l by heme b_h [8]. The slowness of the re-reduction of cytochrome c_1 as compared to the reduction of heme b_h [18,51,54,95–97] indicates, however, that the undocking of the FeS domain happens even later, it seems to correlate with the oxidation of heme b_h, as shown in Fig. 4B (see Sections 2.5.1 and 3.2 for the further consideration of this point).

Elaborated studies in several labs yielded a wealth of functional data on the mobility of the FeS domain and on its interaction with cytochrome b and cytochrome c_1, respectively [77,90,91,98–108]. Particularly, Daldal et al. have shown that the E_m^7 value of the FeS cluster was elevated up to 460 mV in several site-specific mutants of *Rb. capsulatus* even in the absence of stigmatellin-type inhibitors. Correspondingly, it was concluded that the elevated E_m is the intrinsic property of the FeS cluster in the cytochrome b position [109], in support of the earlier guesses [51,92]. EPR studies showed that, unlike the reduced FeS domain that stays docked to cytochrome b, the oxidized FeS domain resides in an alternative, supposedly cytochrome c_1 position [103,105].

---

[1] The cleft between cytochrome b and the FeS domain becomes narrower when the latter docks to cytochrome b (see Fig. 4), so that the hypothetical terms "closed" and "open", which were suggested for two states of center P in the absence of structural information [51], remain valid.

2.4. Ubiquinone processing in the photosynthetic reaction center of Rb. sphaeroides

As described above, the quinol-oxidizing center P of bc_1 provides two binding sites for inhibitors, namely a nonpolar one proximally to heme b_l, and a more polar distal one, on the interface between cytochrome b and FeS_b, (see [1,31,78–81,83] and references cited therein). As noted in the previous section, several authors have considered the possibility that the oxidation of quinol takes place in the distal site, after which the formed neutral semiquinone relocates closer to heme b_l to reduce the latter. It was suggested that the relocation might prevent the escape of the second electron to the FeS cluster (see e.g., [6,8,32,80,110]). A detailed version of such a mechanism has been formulated by Crofts et al. [32,80,110,111]. On presenting their tentative model, Crofts et al. [80] used the analogy with the RC of phototrophic bacteria where the secondary quinone acceptor Q_B is reduced to a quinol Q_BH_2 via a semi-quinone intermediate $Q_B^{\bullet-}$ (see Fig. 3 for the general scheme and [25,27–29] for reviews). The low-temperature X-ray crystallography of the *Rb. sphaeroides* RC has indeed revealed two quinone-binding sites in the Q_B-binding pocket, at the interface of the H- and L-subunits of the RC [24]. To emphasize the functional difference between them, Stowell et al. have denoted them as active and inactive one, respectively [24]). These two quinone-binding sites also differ in their polarity: the active site that interacts with a hydrogen-bonded water cluster penetrating from the outside is apparently more polar.[2] However, the model of quinol oxidation in bc_1 that was suggested by Crofts et al. is not consistent with the situation in the Q_B site of the RC. The semiquinone anion $Q_B^{\bullet-}$ is seen in the polar site, close to the non-heme iron atom [24], opposite to what has been suggested for bc_1. Further on, the lifetime of the $Q_B^{\bullet-}$ semiquinone anion reaches minutes at appropriate conditions [112], which indicates its tight binding by the protein and rules out its movement in the site.

Several mutually compatible schemes, where the initial steps of electron and proton transfer to Q_B were arranged with the displacements of quinone ring, were suggested for the RC of *Rb. sphaeroides* [24–27,61,113] and of *Rps. viridis* [23], respectively. It has been even possible to clarify the sequence of events coupled with the last steps of Q_B turnover, when the second electron is transferred to $Q_B^{\bullet-}$ together with two protons and the formed ubiquinol leaves the binding pocket [26,27,61,114,115]. The available data allow to describe the Q_B turnover in the RC as follows (see Fig. 6):

(1) The high-resolution low-temperature X-ray structure [24] indicates that the molecules of Q_B ubiquinone are distributed between two binding sites in the ground state. To reach a coherency with the further presentation, the distal, nonpolar "inactive" site (see Panel A of Fig. 6) is hereafter denoted as a *stand-by* site, whereas the proximal, polar "active" site is denoted as a *catalytic* site (see Panel B in Fig. 6). The relative occupation of the two sites by ubiquinone seems to differ depending on the preparation studied, conditions, and the length of the ubiquinone tail. In the case of the isolated RC of *Rb. sphaeroides* and at room temperature, ubiquinone is predominantly in the catalytic site [116], although functional evidence of heterogeneity of Q_B can be also found in the literature [117–120]. On temperature decrease, quinone relocates into the stand-by site, as it follows from the earlier functional studies [121] and from the low-temperature crystal structure of the RC [24]. In the case of crystal structures of the *Rps. viridis* RC, the short-tail ubiquinone Q-2 was seen predominantly in the catalytic site, while the native long-tail Q-7 occupied the stand-by position [23]. Apparently, the affinity of the tail to the hydrophobic environment affects the ubiquinone distribution between the two binding sites. When the RCs of *Rb. sphaeroides* were studied in native chromatophore membranes, ubiquinone seemed to be distributed between the two binding sites [27,113,122]. Apparently, the two ubiquinone positions are almost isoenergetic [25]. Correspondingly, there is some evidence that a partial relocation of Q_B molecules into the catalytic site takes place already in response to the reduction of Q_A [123,124].

(2) When Q_B is in the stand-by site, its C4 carbonyl forms a hydrogen bond with the backbone nitrogen of the Ile-224 of the L subunit (Ile-L224, see panel A in Fig. 6).

(3) In the catalytic site, as shown in panel B of Fig. 6, the quinone ring makes a 180° twist and comes ~5 Å closer to the conserved Glu-L212 and His-L190 [24]. The latter residue ligates the non-heme iron atom. In this conformation, the C1-carbonyl of Q_B forms a hydrogen bond with Ile-L224 whereas the C4 carbonyl is hydrogen bonded to His-L190. Based on the structural [125,126] and functional evidence [119,120], an additional (weak) hydrogen bond between Glu-L212 and the C3-methoxy oxygen of Q_B was suggested [25,113]; such an interaction could account for the high apparent pK of Glu-L212 (pK_{212}) of ~10.0 [127]. In support of this guess, MD simulations [128,129] and electrostatic calculations [130] indicated that the binding of Q_B in the catalytic position correlated with a protonated state of the Glu-L212 residue [130].

(4) The ET from $Q_A^{\bullet-}$ to Q_B results in a formation of a tightly bound semiquinone anion $Q_B^{\bullet-}$. The respective X-ray structure (see Panel C of Fig. 6) shows that the whole $Q_B^{\bullet-}$ population is now in the catalytic site [24]. MD simulations indicated that the $Q_B^{\bullet-}$ semiquinone is essentially stabilized by its interaction with iron [131]. The X-ray structure of the RC with a light-trapped $Q_B^{\bullet-}$ shows that he latter is also

---

[2] Contrary to bc_1, the polar Q_B-binding site in the RC is customarily called the proximal one because it is closer to the primary quinone Q_A, the electron donor to Q_B; correspondingly, the nonpolar Q_B-binding site is called the distal one.

Fig. 6. Mechanistic scheme of ubiquinone reduction in the RC of *Rb. sphaeroides* (modified from Fig. 7 in [26]). The Q_B binding site is shown rotated by approximately 180° as compared to that in Fig. 3. Correspondingly, the electron is delivered to Q_B from the right side, via His-L190 residue. Element color code: oxygen, red; nitrogen, blue; hydrogen, where shown, yellow; iron, violet. Hydrogen bonds are depicted by dashed lines. (A) The position of Q_B in the distal site as seen in the low-temperature dark-adapted RC structure (PDB entry 1AIJ [24]). (B) The proximal position of Q_B in the catalytic site as seen in the room temperature RC structure (PDB entry 2RCR [126]). (C) The "semiquinone" position of $Q_B^{\bullet-}$, as seen in the low-temperature light-adapted RC structure with a trapped $Q_B^{\bullet-}$ (PDB entry 1AIG [24]). (D) The position of Q_BH^- as modeled after Lancaster and Michel [23] from the crystal structure of the stigmatellin-containing RC of *Rps. viridis*. (E) The "detached" Q_BH_2 is tentatively shown on its way towards the stand-by "quinol" position, before the propeller twist. The hydrogen bond of carbonyl O4 with His-L190 is already broken but the water bridge between Glu-L212 and His-L190 is not formed yet. (F) Ubiquinol Q_BH_2 position in the stand-by site as modeled along the X-ray structure of the *Rb. sphaeroides* RCs, which were crystallized in the presence of sodium ascorbate (PDB entry 1PCR [135]).

stabilized by hydrogen bonds of the C1-carbonyl with Ser-223, Ile-L224, and Gly-225, of the C4-carbonyl with His-L190, and of the C2-methoxy group with Gly-L225 and, perhaps, Thr-L226. The negative charge of $Q_B^{\bullet-}$ shifts pK_{212} to >12.0 [132].

(5) The transfers of the second electron and of the first proton to $Q_B^{\bullet-}$ are tightly coupled. As depicted in Fig. 3,

protons enter the RC via a histidine-rich patch that can be blocked by Zn^{2+} ions (see [28] for a review). The fast protonation of $Q_B^{\bullet-}$ to $Q_BH^{\bullet}$ is followed by a rate-limiting ET reaction [28,114]. The formed ubiquinone-anion Q_BH^- remains bound by the RC [133]. As it is depicted in Panel D of Fig. 6, Q_BH^- is believed to bind in the catalytic site similarly to stigmatellin, which is assumed to be an analogue

of a ubiquinol–anion (see [23] and Fig. 9 in Section 3.1 below).

(6) The second proton is likely to be donated to Q_BH^- by Glu-L212 [127,134]. The transfer of the second proton proceeds with a high activation energy (E_a) of approximately 60 kJ/mol [115]. According to the kinetic analysis [26], this reaction step is governed by the detachment of the quinol ring from His-L190 and by its rotational movement towards the stand-by site, where the ubiquinol Q_BH_2 is seen in the respective crystal structure (see panel E of Fig. 6 and [135]). Upon this ubiquinol retreat, the water molecules enter the Q_B pocket and form a bridge between Glu-L212 and His-L190. As long as Glu-L212 is involved in this bridge as a hydrogen bond acceptor, its pK_{212} dramatically decreases, so that the protonation of Q_BH^- to Q_BH_2 by Glu-L212 becomes irreversible [25,26]. The MD simulations essentially confirmed this scenario [129].

Hence, the proximal Q_B-binding site of the RC, which is formed by His-L190 connected with an iron atom, binds the charged species, namely $Q_B^{\bullet-}$ and Q_BH^-, and serves as the *catalytic* center where the reactions of reduction and protonation take place. The alternative site binds the uncharged species Q_B and Q_BH_2 and serves as a *stand-by* position for a quinone/quinol molecule. The highest activation barriers on ubiquinone reduction seem to be coupled with the journeys of the quinone ring between the stand-by and catalytic sites [26,27,61,113,115,122]. It is likely that a prompt relocation of the freshly formed ubiquinol into the stand-by site prevents the potentially detrimental reversion of the reaction.

2.5. The catalytic cycle of ubiquinol oxidation by the cytochrome bc1 complex as a reversal of the ubiquinone reduction cycle in the RC

In the previous section, the catalytic cycle of Q_B was described in such detail because just the reversal of this cycle and its application to the bc_1 can yield a coherent ubiquinol oxidation picture that is in agreement with available data. The similarity between the Q_B site of the RC and the center P of bc_1 is not limited to the presence of two quinone-binding loci and of an iron atom in the vicinity. The high-resolution X-ray structure of the yeast bc_1 [9] shows stigmatellin, a supposed analogue of a ubiquinol-anion [23], bound between His-181 of the Rieske protein and Glu-272 of cytochrome b. This arrangement resembles the situation in the RC where His-L190 and Glu-L212 are involved both in Q_B binding and stabilization of the $Q_B^{\bullet-}$ semiquinone (see Fig. 6 in Section 2.4 and also Fig. 9 in Section 3.1 below). The list of analogies can be continued, but instead, it seems worthy to consider what happens if the cycle of ubiquinone reduction in the RC, as depicted in Fig. 6 and as described above, is "turned around" in the center P of bc_1, as depicted in Fig. 7 and described below.

2.5.1. Mechanistic scheme of ubiquinol oxidation

Fig. 7 shows a hypothetical scheme of ubiquinol oxidation in bc_1. Its relation to other tentative schemes of center P operation is discussed in Section 4. For coherency with previous models, the avian numeration of the key residues is used. The Glu-272 of the avian cytochrome b corresponds to Glu-271 of beef bc_1, Glu-272 of yeast bc_1 and Glu-295 of *Rb. capsulatus* bc_1. The counterparts of His-161 in avian bc_1 are His-161 in beef bc_1, His-181 in yeast bc_1, and His-156 in the bc_1 of *Rb. capsulatus*.

The key feature of the scheme is the involvement of two binding sites for the neutral ubiquinone/ubiquinol molecules but of only one binding locus for the anionic forms of ubiquinol and of ubisemiquinone.

(1) The cycle starts from a ubiquinol Q_PH_2 residing within cytochrome b (Panel A of Fig. 7). Most likely, Q_PH_2 resides proximally to heme b_l, in the position of Pm-type inhibitors (see Section 2.2 above). It is noteworthy that a non-oxidizable ubiquinol(!) derivative TMDMP has been reported to bind close to the myxothiazol-binding pad in the respective crystal structure [81]. As well, the photoaffinity labeling of the bovine bc_1 by ubiquinone analogue yielded crosslinks with the amino acid residues of the cd1 helix that is crucial for binding of the myxothiazol-type inhibitors (see [83] and Section 2.3 above), but not with the residues of the ef loop, which is crucial for binding of stigmatellin or UHDBT. The ubiquinol proper, however, is not seen in this position in the crystal structures. Therefore, it cannot be completely ruled out that the only stable quinol/quinone binding site is in the center N, which is occupied in the X-ray structures, and that the binding site of Pm-type inhibitors is only transiently "visited" by a ubiquinol molecule upon its re-location from center N into the catalytic site in center P.

(2) The catalytic site is formed at the interface of cytochrome b after docking of the FeS domain and corresponds to the binding site of the Pf-type inhibitors (see panel B of Fig 7, Section 2.2 above, and refs. [9,31,83]). The EPR data indicate that the affinity of the oxidized FeS domain to the docking interface of cytochrome b is low [103]. Still ubiquinol does bind to the oxidized FeS domain; the stigmatellin- and UHDBT-containing crystal structures of bc_1 allowed several authors to model how ubiquinol forms a hydrogen bond with the His-161 residue of the Rieske protein [9,72,82,136], as it is depicted in panel B of Fig. 7. To form this bond, His-161 has to be deprotonated. The available estimates give values in the range of 6.0–8.0 for the apparent pK of this histidine residue [82,92,137–140]. It was argued [9,72,82], based on the inhibitor-containing crystal structures of bc_1, that the second hydroxyl group of ubiquinol forms a hydrogen bond with Glu-272 of cytochrome b (as it is shown in panel B of Fig. 7).

(3) In almost all current models, the oxidation of Q_PH_2 to ubisemiquinone by the FeS cluster is coupled to its deprotonation to a ubiquinol anion (see panel C of Fig. 7). As argued by Rich, the redox potential of the QH_2/QH_2^+ couple is >850 mV, therefore the ubiquinone-anion Q_PH^-, with estimated E_m^7 of ~190 mV, is the form that can be
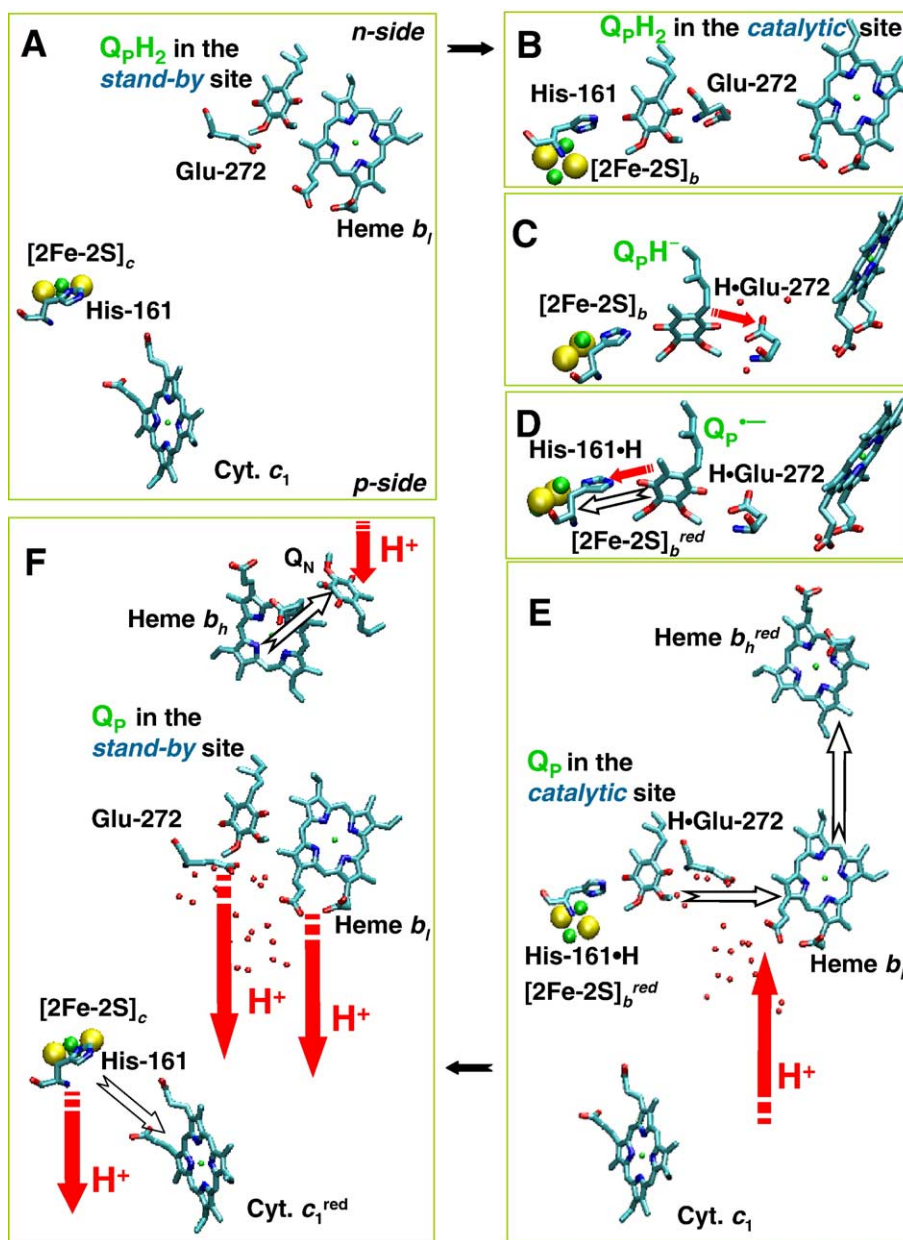
Fig. 7. Tentative scheme of ubiquinol oxidation by bc_1. Element color code: carbon, cyan; oxygen, red; nitrogen, blue; iron, green; sulphur, yellow. Only the reduced states of redox cofactors are indexed. Red arrows, proton transfer events; white arrows, ET events. Figure was produced with the help of the VMD software package [216]. (A) Q_PH_2 is shown in the stand-by site and the FeS cluster in the FeS$_c$ position. The 1BCC PDB entry [6] was used for modeling; the hypothetical position of Q_PH_2 close to heme b_l is based in Fig. 7 from [81]; (B) Q_PH_2 moves into the catalytic site at the interface with the docked FeS cluster; (C) Q_PH^- formation in the catalytic site; (D) $Q_P^{•-}$ formation in the catalytic site. The stigmatellin-containing structure of the yeast bc_1 (PDB entry 1KYO [10]) where stigmatellin was replaced by a ubiquinone ring was used for panels (B)–(D). Although ubiquinol is shown directly bound to His-161 and Glu-272, respectively, a participation of water molecules, which are depicted in panel C, in the ubiquinol binding cannot be excluded. (E) Oxidation of $Q_P^{•-}$ to Q_P and reduction of heme b_l; here Glu-272 turns towards heme b_l whereas the FeS cluster remains docked to cytochrome b, and Q_P stays in the catalytic site. The conformation of Glu-272 was taken from the bc_1 structure of Iwata et al. (PDB entry 1BGY [7]), while the position of Q_P was modeled from the stigmatellin-containing structure of the yeast bc_1 (PDB entry 1KYO [10]). (F) Heme b_h oxidation that is accompanied by the FeS$_b$ → FeS$_c$ transition, cytochrome c_1 re-reduction, and the major electrogenic reaction (see Sections 2.1., 2.5.1. and 3.2. for details). The 1BCC PDB entry [6] was used for modeling; the position of the ubiquinone in center N was taken from the high-resolution structure of the yeast bc_1 (PDB entry 1EZV [9]). For other details, see Section 2.5.1.

oxidized in biological ET [141]. The pK of the QH_2/QH^- couple, deduced from model systems [141] and from the properties of Q_BH_2 in the RC [26,142], is expected in the range of 8.5–11.0. At least two tentative reaction routes could lead to a ubisemiquinone in center P:

(i) In one mechanism, the relocation of the first proton from Q_PH_2 to His-161 of the FeS domain is followed by the electron transfer from Q_PH^- to the FeS cluster yielding a neutral ubisemiquinone (see e.g., [1,19,32]). In this mechanism, which can be named "FeS-first", no genuine Q_PH^-

anion is formed; the first proton does not go away, but just shifts along the hydrogen bond between Q_PH_2 and His-161 by approximately 1 Å. Therefore it remains unclear whether this minor proton shift is sufficient to decrease the oxidizing potential of Q_PH_2 from the estimated >850 mV to an acceptably low value. The formed neutral semiquinone $Q_PH^\bullet$ is likely to give away the proton (as long as the pK of the $Q_PH^\bullet/Q_P^{\bullet-}$ couple is expected to be on the order of 5.0, see the considerations below, in Section 4.1), leaving a ubisemiquinone anion radical $Q_P^{\bullet-}$ in the catalytic center. The most probable acceptor of the second proton is then the Glu-272 residue of cytochrome b [19].

(ii) Alternatively, it is imaginable that Glu-272 of cytochrome b might serve as an acceptor of the first proton ("Glu-272-first" mechanism). Indeed, Covian and Moreno-Sanchez have shown that quinol binding to bc_1 requires a de-protonated state of a group with pK of 5.2–5.7 and attributed this group to Glu-272 [139]. The latter residue can attain two different configurations (see Fig. 7 and also Fig. 4 in Section 2.2): while in the stigmatellin-containing bc_1 structure Glu-272 forms a hydrogen bond with the inhibitor [9], in those X-ray structures of bc_1 where center P is empty [7,72], the side chain of Glu-272 points towards the heme b_l (see Fig. 9 in Section 3.2. below). Thus, Glu-272 shuttles between two conformational sub-states, turning either towards the FeS cluster on ubiquinol binding (Glu-272$_{FeS}$) or towards heme b_l on the retreat of the quinone ring (Glu-272$_{bl}$) (see refs. [19,72]). Because the Glu-272$_{FeS}$ ↔ Glu-272$_{bl}$ equilibrium is shifted to the right when center P is empty [7,72], the estimate of the functional pK, as obtained by Covian and Moreno-Sanchez [139], relates apparently to Glu-272$_{bl}$. The yet unknown functional pK of Glu-272$_{FeS}$ in the presence of quinol/semiquinone is expected to be higher than that of Glu-272$_{bl}$ because the polarity of the pocket is likely to decrease with the intrusion of the ubiquinol ring and the water retreat. The example of the RC shows that the functional pK value of Glu-L212 residue interacting with the Q_B ring is about 9.0–10.0 [127,143]. The pK value of the proton-transporting Glu-286 in the cytochrome c oxidase has been estimated as high as 9.4 (see [144] and references therein). If the functional pK of Glu-272$_{FeS}$ is compatibly high, this residue can outdo His-161 in accepting the first proton from Q_PH_2 to yield a Q_PH^- anion (see panel C of Fig. 7). In the "Glu-272-first" mechanism, a subsequent coupled transfer of an electron and a proton from Q_PH^- to the FeS domain would yield a bound $Q_P^{\bullet-}$ semiquinone anion in the catalytic site, so that at this point of the catalytic cycle, the two tentative mechanisms converge (panel D of Fig. 7). In fact, the Glu-272 residue, which is halfway between two quinol-binding sites, is likely to encounter the ubiquinol *before* His-161. By analogy with the Q_B turnover, it is expected that the iron-containing catalytic site has high (electrostatic) affinity for negatively charged $Q_PH^-/Q_P^{\bullet-}$ species. Then, by accepting the first proton, Glu-272 might facilitate the formation of a histidine-mediated complex between the ubiquinol-anion and the *oxidized* FeS cluster. It is noteworthy that in this case, which is depicted in Fig. 7, the catalytic cycle of ubiquinol oxidation represents an *exact* reversion of the ubiquinone reduction cycle in the RC (cf. with Fig. 6).

(iii) Finally, it is also imaginable that proton attraction by both Glu-272 and His-161 is needed to promote a prompt oxidation of ubiquinol by the FeS cluster (see e.g., [136]). Resolving this question would require further experimental studies.

By analogy with $Q_B^{\bullet-}$ in the RC, a tight binding of the $Q_P^{\bullet-}$ semiquinone to the reduced FeS domain is expected. Such a binding, on one hand, would keep the reduced FeS domain in the cytochrome b position and prevent the escape of the second electron to the FeS cluster (see also Section 3.1 below) and, on the other hand, would make the semiquinone EPR invisible due to its antiferromagnetic interaction with the iron (see refs. [92,145] and the discussion in Section 4.4).

(4) The redox potential of the semiquinone in center P is likely to resemble those of $Q_B^{\bullet-}$ or $Q_A^{\bullet-}$ in the RC, that is, to be in the range of −200/−50 mV [146–150]. Indeed, the polarity of the environment resembles that in the quinone-binding sites of the RC, not to mention the similarity between the putative ligands of $Q_P^{\bullet-}$ and the intimate neighbors of $Q_B^{\bullet-}$. Because of the ability of the $Q_P^{\bullet-}$ semiquinone to reduce oxygen at steady state [151], the most realistic estimate range is −200/−150 mV (The equilibrium $Q^{\bullet-} + O_2 \leftrightarrow Q + Q_2^{\bullet-}$ is shifted to the right already at $E_m(Q/Q^{\bullet-}) < -150$ mV [152]). This value is low enough to enable the reduction of heme b_l. The $Q_P^{\bullet-} \rightarrow Q_P$ transition is most probably coupled with the rotation of the side chain of the protonated Glu-272 towards heme b_l, as depicted on panel E of Fig. 7. The latter suggestion agrees with the observation that Glu-272 does not form a bond with a deprotonated oxygen atom of a quinone analogue, 5-n-heptyl-6-hydroxy-4,7-dioxobenzothiazole [82]. After turning towards heme b_l, the protonated side chain of Glu-272 contributes to the stabilization of the negative charge at cytochrome b (see also Section 3.3). The negative charge might be also compensated by proton redistribution along the water chain, which connects the heme b_l with the p-surface of the membrane (see Fig. 4A in Section 2.1 and Panel E of Fig. 7). On the next step, electron is transferred towards heme b_h at approximately 2 ms [65,85]. The relatively slow time constant indicates that the reaction proceeds on condition of electrostatic compensation (see Section 2.1).

After the reduction of cytochrome b, a neutral quinone is left in the catalytic site (panel E of Fig. 7). The reduced and protonated FeS domain can now, in principle, undock and move to cytochrome c_1. This seems to happen, however, only in the presence of antimycin (see Sections 2.1 and 3.2). In the intact bc_1, the re-reduction of cytochrome c_1 by electrons coming from ubiquinol is delayed as compared to the reduction of heme b_h both in chromatophores of *Rb. capsulatus* [18,36,48–50,54,59] and in the preparations of isolated mitochondrial bc_1 [65,96,97]. The "trapped"

reduced FeS cluster prevents a futile electron escape from the b-chain into the c-chain (see Section 3.2 for a detailed consideration of this point).

(5) The undocking of the FeS domain and its relocation towards cytochrome c_1 (panel F of Fig. 7) seems to be coupled with the oxidation of heme b_h and ubiquinone reduction in center N [51,54,59]. This suggestion was based on the kinetic correlation between the re-reduction of cytochrome c_1 and the oxidation of heme b_h [36,48–50,54,59,95–97], especially under single-turnover conditions [54] (see a more detailed discussion in Section 3.2). As depicted on panel F of Fig. 7 and in Fig. 4B above, (i) the reduction of a quinone/semiquinone in center N by heme b_h is accompanied by proton binding from the n-side of the membrane; (ii) the pK of the Glu-272 residue decreases to the initial acidic value because no surplus negative charge is left at cytochrome b (see Section 3.3), so that Glu-272 releases its proton, operating as a pK switch (see [25] for definition of a pK-switch); (iii) other protons, which, supposedly, were compensating the negative charge on cytochrome b, are released from the p-side as well; (iv) the reduced and protonated FeS domain moves towards cytochrome c_1, reduces the latter, and deprotonates. The transfer of all these charges across the membrane dielectric, together with the re-orientation of the intra-membrane water dipoles (see Section 2.1), account for a large electrogenic reaction, the rate of which correlates both with the rate of the cytochrome c_1 re-reduction and the rate of proton release into the chromatophore interior [18,54,59]. The (i) kinetic correlation between proton release/voltage generation and cytochrome c_1 re-reduction and the (ii) concurrent slowing of these reactions by Zn^{2+} ions (see Section 2.1 and [54,59]) can be explained as follows. The histidine-rich patch of cytochrome b, which binds Zn^{2+} in the mitochondrial bc_1 [71], can serve, on one hand, as a proton outlet from center P (as discussed in Section 2.1, see Fig. 4) and, on the other hand, can interfere, via the ef loop of cytochrome b, with the movement of the FeS domain to cytochrome c_1 (as discussed in more detail in Section 3.2). The putative molecular mechanisms, which might kinetically couple the electrogenic proton release from center P with the re-reduction of cytochrome c_1 by the FeS domain, are considered in more detail elsewhere in relation to the experimental data on electrogenic proton transfer [54,59].

2.5.2. Rate-limiting step of ubiquinol oxidation

The scheme in Fig. 7 provides a new insight on the possible nature of the rate-determining step in ubiquinol oxidation. In model systems, it has been shown that the rate of quinone oxidation is limited by the formation of a complex between a quinol-anion QH^- and the electron acceptor [153–155]. In the case of bc_1, Crofts et al. have suggested, however, that the partial reaction with the limiting rate and the highest activation energy was the oxidation of the bound ubiquinol to a semiquinone (C → D transition in Fig. 7, see [69,110,156]). Turning to the analogy with the RC, it is worth noting that the

respective reverse $Q_B^{\bullet-} \rightarrow Q_BH^-$ reaction (see the C → D transition in Fig. 6) seems to proceed without relocation of quinone ring [23,26,133] and with an activation energy of only about 10 kJ/mol [115]. There are no evident structural or chemical reasons to expect high activation barrier for the congruent reaction step in bc_1.

Crofts et al. have ruled out the formation of the substrate-enzyme complex as the main activation step because the measured E_a of ubiquinol oxidation was independent of the redox state of the quinone pool and, hence, of the quinol presence in the binding site before the flash [69,110,156]. Thereby, it was presumed that there is a single quinol binding site in center P, on the interface between cytochrome b and the oxidized FeS domain. Alternatively to this view, the scheme in Fig. 7 implies two quinol-binding sites in center P, namely the permanent stand-by site within cytochrome b and a catalytic site, which forms only transiently after the docking of the oxidized FeS domain. A stand-by site for ubiquinol is indispensable because the quinol molecule has to reside somewhere when the FeS domain is not docked to cytochrome b. Correspondingly, the main activation step of ubiquinol oxidation could be coupled with the movement of ubiquinol from this stand-by site into the transiently formed catalytic one and with the formation of a complex between the oxidized FeS domain and the ubiquinol ring. The activation barrier for this reaction would be independent of redox potential because the latter correlates with the incidence of quinol in the stand-by site, but not in the catalytic one, which, under any conditions, forms only transiently. The quinol binding to the FeS domain is coupled with the counter-movements (i) of the quinol ring into the catalytic site and (ii) of the oxidized FeS domain towards cytochrome b. The data on site-specific mutants [109] indicate that the hinge region of the Rieske protein needs to be strained to enable the docking of the FeS domain to cytochrome b ("spring loaded mechanism" [111]). To explain the high E_a value of ubiquinol oxidation, Krishtalik has invoked the necessity to overcome the mutual repulsion of amino acid side chains upon docking of the FeS domain to cytochrome b [157]. Moreover, the side chain of Glu-272 has to turn towards the FeS cluster upon quinol binding. All these reactions can account for a relatively high E_a value. The rate of the quinol oxidation, if limited by the docking of the FeS domain, would depend on viscosity, in agreement with recent observations of Cramer et al. made with the chloroplast bf complex [158]. The suggestion is also corroborated by the observation of Yu et al. who have found that the activation energy of the steady bc_1 turnover correlates with the rigidity of the hinge region of the Rieske protein [98]. In the *Rb. sphaeroides* RC, exactly the considered reaction, although going in the opposite direction, is characterized by the highest activation energy of 60 kJ/mol and is the rate-limiting step of the whole Q_B turnover, at least at $t < 20°C$ [26,115]. Although the $Q_BH^- \rightarrow Q_BH_2$

reaction in the RC is coupled with a proton transfer event, its activation energy was shown to be independent of pH at $6.0 < pH < 8.1$ [115], which indicates that proton transfer per se was not limiting. This situation again resembles the situation in bc_1, where the E_a value of quinol oxidation in response to a single flash was shown to be pH-independent in the range of $5.5 < pH < 9$ [69].

Assuming that stigmatellin, in the X-ray structures of bc_1, occupies the site where the $Q_P^{\bullet-}$ semiquinone is bound, the edge-to-edge distance between $Q_P^{\bullet-}$ in the catalytic site and heme b_1 can be expected to be about 11 Å. From the empirical rate/distance dependence for ET in proteins, as put forward by Dutton et al. [62,159] and as given in Section 2.1, the time constant of semiquinone $Q_P^{\bullet-}$ oxidation by heme b_1 can be predicted to be $\leq 10^{-5}$ s under the assumptions that (i) the ΔG value of the reaction is about $-100/0$ meV [69], and (ii) the value of λ is about 1.0 eV, which is typical for proteins [29,114,157,159,160]. This estimate is compatible with the time constant of 3 μs, as found for the ET between $Q_A^{\bullet-}$ and Q_B, over the edge-to-edge distance of 13 Å, in the RC of *Rb. sphaeroides* [161]. Hence, the oxidation of the $Q_P^{\bullet-}$ semiquinone in the catalytic site by heme b_1 is expected to be fast enough and not to hamper the steady enzyme turnover by semiquinone accumulation in center *P*. Hence, there is no need to invoke a relocation of a semiquinone closer to heme b_1 as suggested in [32]. The actual rate of heme b_1 reduction is slower than

estimated above, ∼250 μs, but it is apparently limited by the preceding reaction steps [65].

2.5.3. Energy profile of ubiquinol oxidation

The corresponding energy diagram is depicted in Fig. 8. Here, the first reaction step can be written as

$$Q_P H_2 + FeS^{ox} + b_1^{ox} b_h^{ox} \rightarrow Q_P H^- \cdot H^+ FeS_b^{ox} b_1^{ox} b_h^{ox} \tag{1}$$
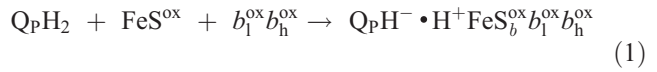
where the first proton (H^+) is accepted either by His-161 residue of the FeS domain or by Glu-272 residue of cytochrome *b* (see the considerations in Section 2.5.1). Although the electrostatic attraction between QH^- and the iron atom(s) might contribute to the "trapping" of the FeS domain, the available structural and functional data indicate that the affinity of the *oxidized* FeS domain to the docking site at cytochrome *b* is low [103,109,162]. Therefore the $Q_P H^- \cdot H^+ FeS_b^{ox} b_1^{ox} b_h^{ox}$ state, an unstable intermediate, is placed high on the energy diagram (see Fig. 8). The top of the activation barrier corresponds to the $Q_P H_2 \cdot FeS_b^{ox} b_1^{ox} b_h^{ox}$ state, which is supposed to be extremely unstable (this state is shadowed in Fig. 8). Correspondingly, the reaction (1) would be endothermic and would account for the major part of the activation barrier of the overall transition (E_a^{conf}).
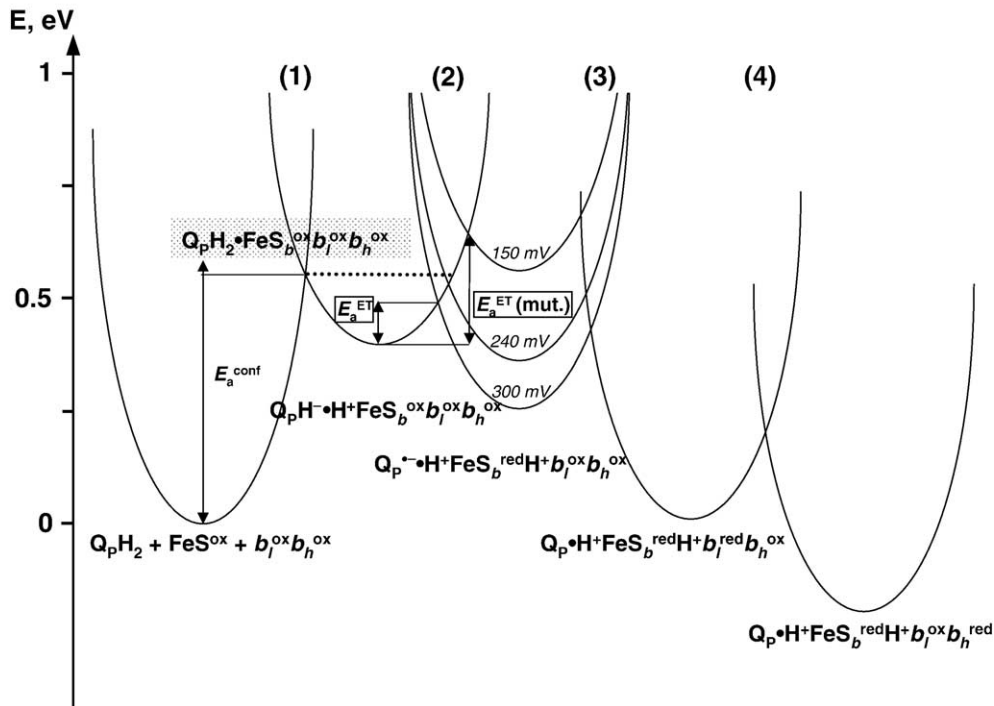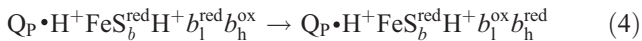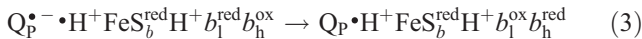

Fig. 8. Energy diagram of quinol oxidation in center *P* of bc_1. See Section 2.5.3. for details. The dotted line marks, for convenience, the activation barrier of the $Q_P H_2$–FeS complex formation in reaction (1). Besides the energy term of the $Q_P^{\bullet-} \cdot H^+ FeS_b^{red} H^+ b_1^{ox} b_h^{ox}$ state in the wild type with a E_m^7 value of 300 mV, the respective traces for mutants with lower E_m^7 values of 240 and 150 mV are shown to illustrate how the ubiquinol oxidation rate may depend on the E_m value of the FeS cluster (see text for details). An approximate energy scale is shown.

The next step is the reduction and protonation of the FeS domain:

$$Q_P H^- \cdot H^+ FeS_b^{ox} b_l^{ox} b_h^{ox} \rightarrow Q_P^{\bullet -} \cdot H^+ FeS_b^{red} H^+ b_l^{ox} b_h^{ox} \qquad (2)$$
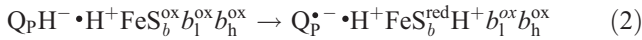
This reaction contributes to the stabilization of the FeS domain in the cytochrome b position as long as the reduced FeS domain, unlike the oxidized one, shows affinity to the docking site at cytochrome b [103,106,162]. As well, the ~150 mV increase in the E_m^7 value of the FeS cluster upon its docking to cytochrome b, as shown for the *Rb. sphaeroides* bc_1 ([107,109], see also Section 3.2), would additionally stabilize the $Q_P^{\bullet -} \cdot H^+ FeS_b^{red} H^+ b_l^{ox} b_h^{ox}$ state. In this case one can speak about a kinetic trapping of the FeS domain by the reduction of its FeS cluster, similarly to the kinetic trapping of oxygen in the cytochrome c oxidase [163]. This reaction step (2) is exothermic and drives the quinol oxidation. This ET reaction is characterized by its characteristic activation energy, E_a^{ET}, which, together with E_a^{conf}, account for the overall activation barrier of the quinol oxidation (see Fig. 8). The $Q_P^{\bullet -} \cdot H^+ FeS_b^{red} H^+ b_l^{ox} b_h^{ox}$ state can be considered as a metastable intermediate as long as it can manifest itself via the interaction with oxygen and superoxide generation [87,151,164,165].

The following electron transfer steps, first from $Q_P^{\bullet -}$ to heme b_l (reaction (3)), and then from heme b_l to heme b_h (reaction (4)) contribute to the further stabilization of the system:

$$Q_P^{\bullet -} \cdot H^+ FeS_b^{red} H^+ b_l^{red} b_h^{ox} \rightarrow Q_P \cdot H^+ FeS_b^{red} H^+ b_l^{ox} b_h^{red} \qquad (3)$$

$$Q_P \cdot H^+ FeS_b^{red} H^+ b_l^{red} b_h^{ox} \rightarrow Q_P \cdot H^+ FeS_b^{red} H^+ b_l^{ox} b_h^{red} \qquad (4)$$

The rate of ubiquinol oxidation can be then written as:

$$v \approx A \cdot e^{-Ea/RT} \cdot [Q_P H_2] \cdot [FeS^{ox} b_l^{ox}] \qquad (5)$$

where $Ae^{-Ea/RT}$ is a pH-independent activation term (rate constant), $[Q_P H_2]$ is a redox-dependent term reflecting the amount of available ubiquinol, and $[FeS^{ox} b_l^{ox}]$ is a pH- and redox-dependent term that reflects the availability of bc_1 complexes with oxidized and de-protonated electron/proton acceptors in the appropriate conformational states. In other terms, ubiquinol binding and oxidation could proceed if the FeS cluster and heme b_l are oxidized, the immediate acceptors of protons from $Q_P H_2$ (His-161 of FeS and Glu-272 of cytochrome b in our scheme) are de-protonated, the FeS domain is in the FeS_b state, and the Glu-272 residue is in the Glu-272$_{FeS}$ conformation. It is noteworthy that the requirement of de-protonated proton acceptors implies that the rate of the quinol oxidation, contrary to E_a, would decrease with acidification, in agreement with experimental observations [166].

With site-specific mutants, it has been shown that the rate of the heme b_h reduction slowed down with the decrease in the midpoint potential of the FeS cluster both in chromatophores of *Rb. sphaeroides* in the presence on antimycin [166] and in the isolated preparations of the yeast bc_1, which were studied in a pre-steady state mode [167]. The slowing, however, was weak as the E_m^7 value of the FeS cluster was decreased from approximately 300 mV to approximately 240 mV, but became more pronounced with the further decrease in E_m^7 [166,167]. The energy diagram in Fig. 8 shows how the relation between E_a^{conf} and E_a^{ET} can determine whether the reaction rate depends on the E_m value of the FeS cluster or not. No notable dependence on ΔG^{ET} is expected as long as the activation barrier of the ET reaction (2), E_a^{ET} in Fig. 8, stays lower than the activation barrier of the reaction (1) (this situation would correspond to a moderate decrease in the E_m value of the FeS cluster). Upon the further decrease in the E_m value of the FeS cluster, the activation barrier of the ET reaction (2) grows (see E_a^{ET}(mut) in Fig. 8) and can become higher that that of the reaction (1). Then the reaction (2) would contribute to the activation barrier of ubiquinol oxidation, and a Marcus-type dependence on ΔG^{ET}, with reaction rate changing by a factor of 10 per 120 mV change in ΔG^{ET} [168], could be expected, in agreement with experimental observations [166,167].

3. Protection from short-circuits in the cytochrome bc_1 complex

As it has been already discussed in the literature (see e.g., [104]), the major task of the bc_1 machinery is to avoid an "energy collapse" that would happen if both electrons slip from $Q_P H_2$ into the high potential c-chain (the possible short-circuit routes are considered in Refs. [20,165]). The mechanistic scheme of quinol oxidation in Fig. 7 implies three traits that can protect the bc_1 from short-circuiting.

3.1. Binding of $Q_P^{\bullet -}$ to the FeS domain

By analogy with the $Q_B^{\bullet -}$ binding in the RC, the $Q_P^{\bullet -}$ semiquinone is expected to be tightly bound/stabilized by its interaction with the iron of the FeS cluster [51,92,137]. Fig. 9 compares the relative arrangements of iron and stigmatellin in the Q_B-binding site of the *Rps. viridis* RC [169] and in the center P of the yeast bc_1 [9] (because no structures of bc_1 with a semiquinone in center P are available, the stigmatellin is considered as an analogue of an anionic semiquinone/ubiquinol [169]). The structural similarity is evident: in both cases the interaction with iron is mediated by a histidine ring, with the same distance of 6.67 Å between the iron atom and the nearest oxygen of stigmatellin. Molecular dynamics simulations of the RC showed a strong interaction between the negatively charged Q_B species and the iron atom [131], which, apparently, accounts for the high stabilization of the $Q_B^{\bullet -}$ semiquinone. This stabilization manifests itself in the long lifetime of $Q_B^{\bullet -}$ that can reach minutes under appropriate conditions [112]. The structural congruency, as seen in Fig. 9, implies a comparably tight binding of the semiquinone to the FeS domain in bc_1. The bound $Q_P^{\bullet -}$ is likely to "hold" the reduced FeS domain and prevent its relocation towards
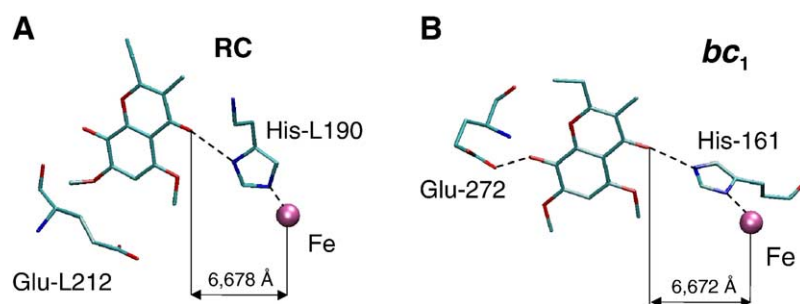
Fig. 9. Binding of stigmatellin in the Q_B site of the RC (A) and in the center P of bc_1 (B). Color code as in Fig. 3. (A) Stigmatellin binding in the RC of *Rps. viridis* as seen in the respective crystal structure (PDB entry 1PRC [23]). (B) Stigmatellin binding in center P of yeast bc_1 as seen in the respective crystal structure (PDB entry 1KYO [10]).

cytochrome c_1. Then, the second electron is compelled to reduce heme b_1.

3.2. FeS-lock mechanism

As noted in Sections 2.1 and 2.5.1, the re-reduction of cytochrome c_1 by electrons coming from ubiquinol is delayed as compared to the reduction of heme b_h. Hence, the FeS domain seems to stay transiently locked in the cytochrome b position even after the $Q_P^{\bullet-}$ semiquinone is oxidized to Q_P. This "FeS-lock" might be important under the coupled conditions, where the oxidation of ubiquinol is impeded by the backpressure from the membrane potential. Indeed, the small edge-to-edge distances of <11 Å between heme b_1, heme b_h and Q_N as well as minor differences in their midpoint potentials imply that an electron, after entering the b-chain, remains essentially equilibrated between the low-potential redox components of bc_1. Moreover, edge-to-edge distance between two b_1 hemes in the bc_1 dimer is also <11 Å, so that electrons, according to the rate/distance dependence for biological ET [159], are likely to equilibrate between two low-potential ET branches of the bc_1 dimer on the time scale of the turnover. This possibility of electron exchange between the monomers was considered by several authors (see e.g., [5,170–173]) and was explicitly incorporated in some structure-based schemes of the dimeric Q-cycle [18,20]. Then, if the FeS domain is not constrained in its shuttling between cytochrome c_1 and cytochrome b, the electron can be driven back into center P by $\Delta\psi$ and eventually can even escape via an oxidized FeS domain (e.g., using a quinone molecule in center P as a ET bridge). Therefore, it seems advantageous to prevent the oxidation of the FeS domain until the turnover of bc_1 reaches some point of "no return". As argued elsewhere [51,54,59], such a point of "no return" might be the oxidation of heme b_h leading to the ubiquinol formation in center N.

The retardation of the cytochrome c_1/f re-reduction as compared to the reduction of cytochrome b seems to be a phenomenon that is common both to bc_1 and to bf complexes. Besides being observed in the flash experiments with phototrophic bacteria [18,36,48–51,54], this phenomenon was also seen in pulsed experiments with the isolated intact mitochondrial bc_1 as studied by stop-flow [95,96] and by using

"caged" ubiquinol [97]. Similar observations were done with the cytochrome bf complexes of green plants [174–177]. In many of these cases, the cytochrome c_1/cytochrome f re-reduction correlated with the oxidation of heme b_h.

In the case of the cytochrome bf complexes, the kinetic mismatch became accepted (see e.g., [1]) after Cramer et al. have provided a key evidence for the absence of a tight coupling between the reduction of cytochrome b, from the one side, and the reduction of cytochrome f and electrogenesis, from the other side. These authors have found out that mutations of amino-acid residues in cytochrome f retarded both the reduction of cytochrome f and the generation of the transmembrane voltage without affecting the rate of cytochrome b reduction. Thereby, the latter reaction was distinctly faster than the former two [178]. Further on, the kinetic discrepancy between cytochrome b reduction and the re-reduction of cytochrome f increased with the increase in the lumenal viscosity [158].

In the case of bc_1, the cause of the kinetic disparity is still under debate (see e.g., [179]). The studies of intact bc_1 under single-turnover conditions, which could be created, even in the absence of antimycin, by substrate shortage [18,96,97,180] or by weak light flash (see Section 2.1 and [51,54,59]), seem to be instrumental in solving this controversy. As well, the addition of Zn^{2+} ions to the intact, membrane-embedded bc_1 of *Rb. capsulatus* increased the kinetic mismatch between the faster reduction of heme b_h and the slower cytochrome c_1 re-reduction and voltage generation up to a factor of ~10 [54,59], making the discrepancy unambiguous (the resultant scheme of a two-step operation of bc_1 is depicted in Fig. 4 and briefly discussed in Sections 2.1 and 2.5.1).

A direct evidence of electron trapping by the FeS domain has been recently obtained by Zhu and co-workers who used ultrafast microfluidic mixer and freeze-quenching device, coupled with EPR (see [65] and Section 2.1). These authors succeeded to determine the pre-steady state kinetic of ubiquinol oxidation. The FeS cluster was reduced, after a 100 μs lag, with half time of 250 μs. A similar reduction kinetic was also observed for cytochrome b_1 indicating simultaneous reduction of both the FeS cluster and heme b_1. The time constants of ~2.5 ms and ~6 ms were observed for the reduction of heme b_h and cytochrome c_1, respectively, in good

correspondence with the respective time constants, as found in the Zn^{2+}-treated chromatophores of *Rb. capsulatus* [54,59].

Mechanistically, the $FeS_b \rightarrow FeS_c$ transition can be retarded in two ways, namely: (i) if the E_m of FeS_b is much higher than that of FeS_c; in this case, the $FeS_b \rightarrow FeS_c$ transition goes energetically uphill and would be retarded even if the intrinsic constant of the $FeS_b \rightarrow FeS_c$ movement is fast; (ii) if the return of the FeS domain into the FeS_c position is conformationally constrained. These two possibilities are not mutually exclusive and there is experimental evidence in favor of both of them, so that most probably some combination of (i) and (ii) is involved. Particularly, Daldal et al. have shown that the E_m^7 value of the FeS cluster was increased, up to 460 mV, in the site-specific mutants of *Rb. capsulatus* with hinge domain of the Rieske protein elongated by the addition of alanine residues [109]. Correspondingly, it was concluded that a tight inhibitor binding is not a precondition for an increase in E_m, and that the elevated E_m is the intrinsic property of the FeS cluster in the cytochrome *b* position [109]. In support of this view, it has been recently shown that even after the extraction of ubiquinone the E_m value of the FeS cluster remained elevated by ~ 50 mV in the alanine mutant [107]. The reason for the E_m elevation might be straightforward. It is well established that the midpoint potentials of the [2Fe–2S] clusters in the Riske-type iron-sulphur proteins increase with the number of hydrogen bonds that stabilize the reduced cluster [140,181]. The docking of the FeS domain to cytochrome *b* implies that the [2Fe–2S] cluster, which is only partially covered by protein, comes into the medium with lower dielectric permittivity (ϵ_{eff}). At lower ϵ_{eff} the hydrogen bonds are expected to strengthen, which would lead to the increase in the E_m value of the cluster.

Darrouzet and Daldal have shown that the *ef* loop of cytochrome *b*, which is shown as a yellow tube in Fig. 4, acts as a barrier that needs to be crossed by the FeS domain on its way to cytochrome c_1 [91], in confirmation of the earlier MD simulations [68]. In the site-specific mutant with an additional alanine residue inserted into the hinge region of the Rieske protein, the oxidation of a RC-generated ubiquinol proceeded normally, but no electron was delivered to cytochrome c_1. The function was, however, partially restored in the double mutants, where the leucine at position 286 in the *ef* loop of cytochrome *b* was replaced with a phenylalanine. Apparently, the *ef* loop prevented the $FeS_b \rightarrow FeS_c$ motion in the single mutant [91]. The picture that emerges from these elaborated studies offers a wide range of possibilities to control the $FeS_b \rightarrow FeS_c$ transition, from the one side, via docking interactions in center *P* and, from the other side, via conformational impact on the hinge region of Rieske protein and/or on the *ef* loop of cytochrome *b*.

The apparent "release" of the FeS-lock in response to a redox reaction in center *N*, and the deactivation of the lock in the presence of antimycin (see Section 2.1, 2.5.1 and [18,51, 54,59,96,97,182]) can be considered as one more evidence of a conformational coupling between centers *N* and *P*. After being put forward in [51], the possibility of such a coupling

was tackled in several publications [18,101,108,136]. Daldal et al. have shown that the cleavage of the Rieske protein at the hinge region by thermolysin depended on the state of center *N* [101]. While in the untreated bc_1, only 50% of the FeS domains were cleavable by thermolysin, in the presence of stigmatellin the cleavage was blocked, and in the presence of antimycin the cleavage was about 80%. Because, as it is known from X-ray data, stigmatellin fixes the FeS domain in the cytochrome *b* position, it could be straightforwardly suggested that the cleavability depended on the position of the FeS domain, so that the protein was accessible to thermolysin only when the FeS domain was close to cytochrome c_1 or stayed in some intermediate position. In this case, the data might indicate that antimycin shifted the $FeS_b \leftrightarrow FeS_c$ equilibrium to the right. The situation, however, was not so simple: the antimycin-treated bc_1 showed a typical $g_x = 1.800$ EPR signal indicating an interaction of the Q_P ubiquinone with a reduced FeS domain in the cytochrome *b* position. Therefore, the authors attributed the enhanced cleavability of the Rieske protein to the antimycin-induced conformational changes in the hinge region proper, which was the target of the protease. It is noteworthy, however, that the cleavage experiments were carried out in the absence of added electron donors, so that one can expect that the FeS cluster was oxidized during the assay. The EPR measurements, from the other side, are routinely conducted with a pre-reduced FeS cluster because the oxidized one is EPR-silent. Unless Q_PH_2 is present, an oxidized FeS domain seems to reside in the cytochrome c_1 position unlike the reduced one, which shows weak affinity to the docking site at cytochrome *b* in the presence of ubiquinone [103,106]. Thus, the data of Daldal et al. might indicate that the position of the *oxidized* FeS domain depends on the presence of antimycin in center *N*. In support of the earlier suggestions of a functionally relevant conformational coupling between centers *N* and *P* [18,51,54,59,96,97,180], Cooley and Daldal have recently shown, by using EPR spectroscopy, that either inhibitor binding or single residue mutation events at the Q_N site altered the interaction of the FeS domain with ubiquinol at the Q_P site in a manner that was dependent upon the nature of interactions at the Q_N pocket [77]. These results of Daldal et al. might be related to the earlier observations (i) on the easier dissociability of the Rieske protein from the isolated bc_1 in the presence of antimycin (see [183] and references cited therein),and (ii) on the propagation of the antimycin-induced conformational change towards heme b_l [184]. An extensive further discussion of how center *N* can be mechanistically coupled to the Rieske protein can be found in [101].

It is noteworthy that even when the FeS-lock is deactivated, the electron divergence in center *P* can be still ensured by the tight semiquinone binding (*vide supra* Section 3.1) and by the involvement of the Glu-272 switch (*vide infra* Section 3.3). It remains unclear, however, whether a bc_1 complex with a deactivated FeS-lock is able to pump protons against the membrane potential backpressure: both the antimycin-treated and the heme b_h-depleted enzymes, in which the FeS-

lock, apparently, does not operate, cannot perform a complete electrogenic turnover.

3.3. "Glu-272" switch

As noted in Section 2.5.1 and depicted in Figs. 4 and 7, the comparative analysis of X-ray structures has shown that the side chain of Glu-272 can turn towards heme b_1 and the water-filled channel that connects the heme with the external water phase [9,72,82]. Correspondingly, it has been speculated that the rotation of Glu-272 is required for proton release into this channel (see [72,82] and comment in Section 2.1). The mobility of Glu-272 might play an even more important role in controlling the events in center P. The FTIR spectroscopy of the *Rb. capsulatus* bc_1 has shown that the reduction of heme b_1 was coupled with the protonation of a carboxy group peaking at 1720 cm^{-1} [67] (in an independent study of *Rb. capsulatus* bc_1 by the ATR-FTIR spectroscopy this peak has been recently confirmed at 1723 cm^{-1} [185]). Because the signal was twice as large at pH 6.5 than at pH 8.7, the pK of this carboxyl was estimated as ~8.7 [67]. From these data, the extent of pK shift at this group in response to heme b_1 reduction can be estimated as >2.5. Taking a value of 8–12 for ϵ_{eff} (see [186,187] for estimates of ϵ_{eff} values inside membrane proteins), the distance between the heme iron and the carboxyl can be estimated from the Coulomb's equation as <8–12 Å. The structure of the *Rb. capsulatus* bc_1 [11] implies that the only carboxyl that is close enough to heme b_1 is the Glu-272 residue when it is turned towards the heme (Glu-272$_{bl}$). Other carboxyls are >20 Å away from heme b_1. It is thinkable that when heme b_1 is pre-reduced at equilibrium, Glu-272 stabilizes the negative charge at the heme by taking a proton from the medium, perhaps, via the water chain (see Fig. 4A). Further on, the same signal at 1720 cm^{-1} has been observed in response to the reduction of heme b_h as well [67]. The heme b_h is 22 Å away from Glu-272 in the crystal structure. Assuming a ϵ_{eff} value of 6–8 for the inner, hydrophobic part of cytochrome b, the energy of electrostatic interaction between heme b_h and Glu-272 can be estimated as about 90 mV, implying a pK shift of 1.5 units at Glu-272 in response to the heme b_h reduction. The smaller pK shift correlates with the observation that when only heme b_h was reduced, the signal at 1720 cm^{-1} was seen at pH 6.5 but not at pH 8.7 [67].[3]

These electrostatic considerations point to a following tentative scenario, which is schematically depicted in Fig. 10. When center P is empty and the hemes of cytochrome b are oxidized, Glu-272 is turned towards heme b_1 in the respective

crystal structures [7,72]. This indicates that the intrinsic Glu-272$_{bl}$ ↔ Glu-272$_{FeS}$ equilibrium (A ↔ B equilibrium in Fig. 10) is shifted to the left, i.e., towards the state A in Fig. 10. With the reduction of the cytochrome b hemes and the expected protonation of Glu-272 the system would get into a state H$^+$Glu-272$_{bl}$ (state C in Fig. 10); thereby, the negative charge at the hemes would further stabilize the H$^+$Glu-272$_{bl}$ state. The ubiquinol binding requires, however, a deprotonated Glu-272$_{FeS}$ residue (state B in Fig. 10). Hence, the binding of a ubiquinol in the catalytic site under the conditions where the hemes of cytochrome b are pre-reduced would require a "diagonal" C → B alteration of the Glu-272 residue (deprotonation + flip, see Fig. 10). This requirement would strongly hamper the binding and oxidation of ubiquinol when cytochrome b is reduced. Although the flips of the Glu-272 side chain proper are expected to happen at pico/nanoseconds (see e.g., [188] for molecular dynamics (MD) simulations of carboxyl side chain mobility), a steady population of the de-protonated form of Glu-272$_{FeS}$, which determines the ubiquinol oxidation rate (see Eq. (5)), would be low.

The here suggested redox-controlled swinging of the Glu-272 side chain resembles two well-studied cases of carboxy side chain mobility in redox enzymes. The first case is the one of the strongly conserved Glu-286 in the cytochrome c oxidase. Here, the comparative analysis of various crystal structures showed that the protonated side chain of Glu-286 might move in response to redox changes in the cytochrome c oxidase and connect thereby the input and output proton channels [144]. The other relevant case is the one of the Asp-15 in ferredoxin I from *Azotobacter vinelandii*. This residue was shown to transfer protons, by a swinging movement, from the water phase towards the μ_2S sulphur atom of the [3Fe−4S] cluster [189]. The MD simulations showed that a reaction mechanism based on a side-chain flipping is effective only as long as two configurations of the side chain are isoenergetic. The enzyme function is effectively blocked if one of the conformations is selectively stabilized and the mobile residue becomes "fixed" [188]. This seems to happen with the protonated Glu-272$_{bl}$ after the complete reduction of cytochrome b.

It is noteworthy to emphasize that the heme b_1-due electrostatic influence, which was discussed above in relation to Glu-272, is not a prerogative of this specific residue, but of any potential proton acceptor located between the quinol ring and heme b_1. This notion might be related to the ubiquinol oxidation by mutants lacking Glu-272 [72] and to the plastoquinol oxidation by the cytochrome bf complex.

3.4. Conformational gating

Hitherto it has been assumed that, besides the considered twists of the side chain of Glu-272, there is no other allosteric impact on the stabilization/binding of the quinol/semiquinone ring in center P either (i) from the reduction of cytochrome b hemes or (ii) from the binding of inhibitors in

---

[3] It is noteworthy that before the bc_1 structure was resolved, Konstantinov has already suggested that variations in the particular pK value of a group X, electrostatically coupled both with heme b_1 and heme b_h, could explain eventual differences in electron/proton coupling in bc_1 of mitochondria and of phototrophic bacteria [221]. The available structural data, as argued above, strongly indicate that this hypothetical group X is likely to be Glu-272. It is noteworthy that the redox-dependence of the FTIR signals at ~1700 cm^{-1}, which correspond to protonated carboxyls, indeed differ between the mitochondrial bc_1 [222] and the bc_1 of *Rb. capsulatus* [67,185].
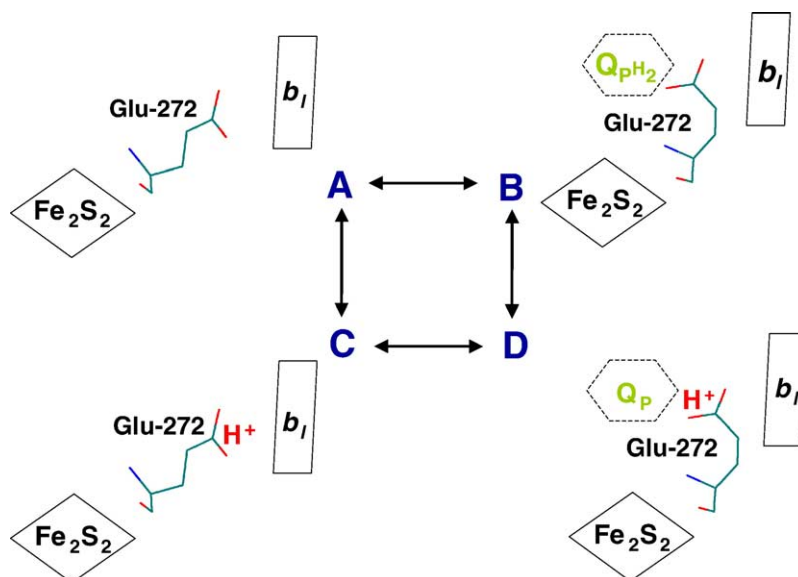
Fig. 10. Simplified square scheme of conformational transitions of the Glu-272 residue in the cytochrome bc_1 complex (see Section 3.3 for details). (A) The catalytic site is empty, the Glu-272 residue is turned towards the oxidized heme b_l; (B) the Glu-272 residue is turned towards the FeS cluster and participates in ubiquinol binding; (C) the reduction of heme b fixes the protonated Glu-272 in the cytochrome b position; this state is highly unfavorable for ubiquinol binding; (D) the stabilization of ubiquinone or semiquinone anion in the catalytic site requires a protonated Glu-272 residue turned towards the FeS domain.

center N. Both assumptions might be wrong. The reduction of cytochrome b is coupled with the relative angular displacement of the hemes [190], which implies a major conformational change. If, due to a conformational change in cytochrome b, the Glu-272 would loose the ability to reach the ubiquinol ring and to form a hydrogen bond with the latter, the ubiquinol oxidation in center P would be efficiently impeded. The same is true for other residues involved in the stabilization of the quinol ring (see e.g., [82]). As mentioned above, the data of Daldal et al. on the higher cleavability of the Rieske protein in the presence of antimycin [101] might indicate that the $FeS_b \leftrightarrow FeS_c$ equilibrium for the oxidized FeS domain is shifted to the right in the presence of this inhibitor. Such a shift would impede the stabilization of quinol/semiquinone in the catalytic site as well. The binding/stabilization of ubiquinol can be also affected by the antimycin-induced long-range conformational interactions in cytochrome b [184]. Cooley and Daldal have concluded in their already cited study of the coupling between centers N and P by means of EPR spectroscopy ([77], see also Section 3.2 above), that "the structure of cytochrome b subunit itself changes as a function of the dynamic events at one side or the other".

4. Comparison of different models of ubiquinol oxidation by the cytochrome bc_1 complex

4.1. Mobility of ubisemiquinone

Concerning the mobility of the ubisemiquinone in center P, the suggested mechanism of ubiquinol oxidation is at odds with models that imply a neutral ubisemiquinone that moves between the two binding sites (see Section 2.3 and [80,110,111]).

Other tentative models of ubiquinol oxidation, however, imply a single binding site for the semiquinone. The earlier insightful model of Link [92] implies a single binding site for an immobile ubisemiquinone. In this model, however, the nature of proton accepting groups was not specified. As well, the recent structure-based models of Hunte et al. [82] and of Berry and Huang [136] imply only one binding site for ubisemiquinone.

The mobility of a ubisemiquinone is expected to depend on its charge. While a relocation of neutral semiquinone between the two binding sites is imaginable, the negatively charged $Q_P^{\cdot-}$ would be tightly bound to the FeS domain by the electrostatic interaction with iron. The pK value of a $Q^{\cdot-}/QH^\cdot$ couple in an aqueous environment has been estimated to be about 5.0 [191]. In agreement with this estimate, the EPR-detectable ubisemiquinones in different membrane proteins, to the best knowledge of the author, showed characteristic EPR and optical spectra of anion-radicals at neutral pH values (see e.g., [192] and references cited therein). The anionic nature of these semiquinones is likely to be due (i) to the abundance of water molecules in the respective binding pockets [9,31,193] and (ii) to the electrostatic influence from positively charged iron atoms, which are usually present in vicinity. The high resolution X-ray structure of bc_1 [9] shows water molecules in center P. The expected, from the stigmatellin binding, position of the $Q_P^{\cdot-}$ semiquinone (cf. Figs. 7 and 9) is 7 Å away from the nearest iron atom of the FeS cluster. The electrostatic influence from iron does shift the pK values of the

histidine ligands of the FeS cluster from ∼14.0 to ∼6.0–9.0 [137,140,181]. A semiquinone in the catalytic site would feel this electrostatic impact of iron as well. Thus, there is no apparent reason to expect a neutral semiquinone in center P under physiological conditions.

4.2. Two binding sites for ubiquinol/ubiquinone

The tentative mechanisms of ubiquinol oxidation, as suggested so far, have considered either (i) a single binding site in center P for neutral ubiquinone/ubiquinol species (see e.g., [19,80,136]) or (ii) two ubiquinone/ubiquinol molecules simultaneously bound with different affinities to two binding sites in center P, as suggested by the double occupancy model [194,195]. Concerning the latter model, the X-ray structures of bc_1 did not show any ubiquinone bound in center P. Crofts et al. have suggested alternative explanation for the EPR data, on which the double occupancy model was based [1,32,80]. However, one has also to take into account the recent indications of the binding of two quinone-like molecules of DBMIB in bf [196] and of two Q_0 ubiquinone molecules in the mitochondrial bc_1 [197]. It is plausible that the center P is large enough to accommodate two quinone rings, especially if tail-less species are involved, as in the works cited above. Still it seems that the available structures of bc_1 do not offer enough space in center P for two single-tailed molecules of ubiquinone getting in and out through the same protein tunnel, not to mention menaquinone, which is even more bulky, but can be efficiently oxidized by the mitochondrial bc_1 [96]. The possibility that a second long-chain quinone can access the center P directly from the phospholipid bilayer, avoiding the protein tunnel, cannot be fully ruled out, especially in the case of the smaller bacterial bc_1. This option, which might be useful in rationalizing bypass ET reactions in bc_1 (see e.g., [164,165]), deserves further clarification.

To the best knowledge of the author, the possibility of a functionally relevant rocking of the same neutral ubiquinol/ubiquinone molecule between the *two* binding sites has not been explicitly addressed so far. It looks like that such a rocking is a distinct feature of the suggested mechanistic model of ubiquinol oxidation by bc_1.

4.3. Proton gating

Deprotonation of ubiquinol has been suggested to be the activation step in at least two models of ubiquinol oxidation [92,198]. The suggestion, on one hand, was based on the model experiments, which have shown that the deprotonation of QH_2 to QH^- is the most probable first step of ubiquinol oxidation [141]. On the other hand, the activation energy of ubiquinol oxidation, as determined for the steady turnover of the mitochondrial bc_1, was shown to decrease with pH [199]. The latter observation has prompted Brandt to hypothesize that the ubiquinol

oxidation is proton-gated, with the FeS center acting as the acceptor of the first proton [198,199]. However, as already noted in Section 2.5.2, the E_a of ubiquinol oxidation, as determined for the *Rb. sphaeroides* bc_1 in single-flash experiments by Crofts et al., found to be independent of pH at $5.5 <$ pH < 9.0 [69].

This disparity between the data obtained at steady state with mitochondrial bc_1 [199] and in flash-experiments with the bc_1 of *Rb. sphaeroides* [69] deserves consideration. One possible solution follows from the scheme in Fig. 7. Here, the flash-induced *reduction* of heme b_h, which was studied by Crofts et al. [69], corresponds to the D → E transition. The steady turnover of bc_1, which was studied by Brandt et al., is, however, kinetically limited upon the later turnover step, which is coupled with the *oxidation* of heme b_h, the re-reduction of cytochrome c_1 and the $\Delta\psi$ generation. This step is the rate limiting one both in coupled mitochondria [200,201] and in chromatophores of *Rb. sphaeroides* [36]. In flash experiments with bc_1 of *Rhodobacter*, the oxidation of heme b_h and the re-reduction of cytochrome c_1 were concomitantly slowed down by the membrane potential [36] and by the ubiquinol shortage [18]. The scheme in Fig. 7 attributes this rate-limiting step to the E → F transition. Upon this step protons are released from bc_1 into the surrounding water phase by Glu-272 of cytochrome b and by His-161 of the Rieske protein (as illustrated by Fig. 4B; see also Section 2.5.1). The activation energy of this proton release could decrease with pH elevation because of gradual deprotonation of proton relay(s) involved. The facilitation of proton ejection at higher pH could decrease the E_a of the overall turnover at steady state.

In earlier work [69], Crofts et al. ruled out the possibility of proton gating because the E_a of ubiquinol oxidation was independent of pH in flash experiments (see above). Thereby, the high E_a of ubiquinol oxidation was attributed to the rate limiting ET reaction (see refs. [69,110] and Section 2.5.2 above). This led, however, to a reorganization energy value of ∼2 eV that was unrealistically high for a ET reaction in protein. To overcome this difficulty, Crofts has recently invoked the participation of protons to explain the high E_a of ubiquinol oxidation [156]. It has been suggested that the transfer of the first electron from Q_PH_2 to the FeS cluster proceeds by proton-coupled electron transfer (PCET) mechanism, so that the activation barrier is partly due to the "uphill" proton transfer from Q_PH_2 to the FeS domain (see Section 2.5.1 for the respective pK estimates). As an analogous case, Crofts considered the coupled transfer of the second electron and the first proton to Q_B in the *Rb. sphaeroides* RC ($Q_B^{\bullet-} \to Q_BH^-$ reaction that corresponds to the C → D transition in Fig. 6). The $Q_B^{\bullet-} \to Q_BH^-$ reaction, however, proceeds not by PCET mechanism but sequentially: the ET takes place only after the $Q_B^{\bullet-}$ semiquinone is protonated to $Q_BH^{\bullet}$ by proton coming from the surface histidine cluster (see Fig. 3 and [28]). Although this "uphill" proton transfer slows the reaction rate, it does not contribute to

the activation barrier, so that the E_a value of this reaction is only about 10 kJ/mol [115]. Hence, the "uphill" proton transfer to $Q_B^{\bullet-}$ along a rather long chain of amino acid residues (see Fig. 3) does not elevate the activation barrier of the reaction. In the case of bc_1, the "uphill" proton transfer corresponds to a proton shift by only 1 Å along a hydrogen bond connecting the bound ubiquinol with the His-161 residue of the Rieske protein. It is unlikely that this reaction can limit the overall transition. The dependence of the ubiquinol oxidation rate on the E_m of the FeS cluster but not on pH (see Section 2.5.3 and references cited therein) also speaks against a genuine PCET mechanism. As well, a rate limitation by PCET mechanism poorly corresponds with the strong dependence of the rate of cytochrome b reduction on the viscosity in the cytochrome bf complex [158]. The correlation between the activation energy of the steady bc_1 turnover and the rigidity of the hinge region of the Rieske protein [98] can be also hardly explained by a rate-limiting PCET mechanism. As well, one would expect a notable H/D isotope effect for a quinol oxidation that is limited by a genuine PCET mechanism [202,203]. The H/D effect, as measured by cytochrome b reduction, was <2.0 in the case of the bf complex of *Chlamydomonas reinhardtii* [204] and ~1.5 in the bc_1 of *Rb. capsulatus* (Klishin and Mulkidjanian, unpublished observations). All these findings are, however, compatible with the formation of the Q_PH_2–FeS complex as the rate-limiting step of ubiquinol oxidation (see Section 2.5.2).

4.4. Semiquinone stabilization

The extent of the $Q_P^{\bullet-}$ semiquinone stabilization is another matter of debate. It is worthwhile to discriminate between thermodynamic and kinetic modes of semiquinone stabilization. A thermodynamically stable semiquinone in center P can be ruled out. Evidently, such a semiquinone with a stability constant $K_s>1$ (see [3] for the definition of K_s) would have midpoint potential above that of the Q_PH_2/Q_P redox pair (~100 mV at pH 7.0 [48]) and would be unable to reduce the b_1 heme. The $Q_P^{\bullet-}$ semiquinone reduces heme b_1 even when the b_h heme is pre-reduced and the E_m^7 of heme b_1 is approximately −100 mV (see Table 1 and [64,85]). Hence, the functional redox potential of the $Q_P^{\bullet-}$ semiquinone can be estimated as <−150 mV at pH 7.0 (see also Section 2.5.1); this redox potential would formally correspond to a stability constant of <10^{-3}. The formal stability constant, however, is defined only for semiquinone molecules interacting in a homogenous solution. The stability of a semiquinone that is occluded in a protein is determined by the ability to exchange electrons with the surrounding. An impediment in electron exchange can lead to the formation of semiquinone, which is unstable thermodynamically, but stable kinetically. This happens in the RC where the $Q_B^{\bullet-}$ semiquinone, although thermodynamically unstable, can live for minutes at least [112,150].

As long as an oxidized heme b_1 is available, the $Q_P^{\bullet-}$ semiquinone can be considered to be unstable both thermodynamically and kinetically because the ET to heme b_1 is faster than the activation step of ubiquinol oxidation (see [65] and the discussion in Section 2.5.2). The reduction of heme b_l, as caused by antimycin treatment or by a membrane potential backpressure, seems to lead, however, to the partial kinetic stabilization of the $Q_P^{\bullet-}$ semiquinone. The (partially) stabilized semiquinone manifests itself by its ability to reduce oxygen to superoxide $Q_2^{\bullet-}$ in a stigmatellin-sensitive reaction (see [151,164,165] and references cited therein). This semiquinone is apparently EPR-silent; the EPR-silence has been explained by the antiferromagnetic coupling between the semiquinone and the reduced FeS cluster (see e.g., [92]). A direct evidences of such silencing were obtained upon the studies of the cytochrome bf complex: first Malkin [205] and then Schoepp et al. [206] have shown by using 2,5-dibromo-3-methyl-6-isopropyl-p-benzoquinone (DBMIB), a quinone analogue which tightly binds to the FeS domain in the plant bf, that the generation of the semiquinone form of DBMIB by redox titration resulted in the loss of the EPR signal; the loss was apparently due to the antiferromagnetic coupling in the semiquinone–Fe^{2+} pair.

4.5. Concerted ubiquinol oxidation

A concerted mechanism has been suggested by several authors for the divergent ubiquinol oxidation by bc_1 (see e.g., [20,85,136,207] and references cited therein). It is useful to discriminate between (i) an *apparently* concerted reaction, where two sequential ET reactions proceed without measurable delay because the overall reaction rate is determined either by the first ET step or even by some preceding event, and (ii) a *genuinely* concerted reaction where two electrons go to different acceptors at once. The above discussed data indicate that ubiquinol is oxidized by bc_1 in an *apparently* corrected way; the reaction rate is then determined either by the formation of a complex between Q_PH_2 (Q_PH^-) and the FeS domain (as argued in Section 2.5.2) or by the oxidation of Q_PH_2 to a semiquinone (as suggested by several authors, see [32,156, 165,208] and references cited therein). The *genuinely* concerted mechanism, although very helpful in rationalizing the electron bifurcation phenomenon [20], seems to be, however, unlikely. The electrochemistry of quinones implies that the oxidation of a Q_PH^- anion to a $Q_PH^{\bullet}$ radical is followed by a deprotonation event because a $QH^{\bullet}$ semiquinone can hardly be directly oxidized to a QH^+ cation (by analogy with the QH_2/QH_2^+ pair (see [141]), the $QH^{\bullet} \to QH^+$ reaction would require an impractically high oxidizing potential). Then, a genuinely concerted reaction of ubiquinol oxidation has to invoke a simultaneous transfer of two electrons and of one proton to different acceptors. To the best knowledge of the author, such a triple concerted reaction does not have precedents in

chemistry. Moreover, from general considerations, a large kinetic isotope effect is expected for such a reaction because of proton involvement, in contrast to available data discussed in the previous section. A moderate H/D isotope effect is, however, compatible with the limitation of the reaction by a conformational change (see Section 2.5.2 above).

Turning to the chemical definition, "two or more primitive changes are said to be concerted if they occur within the same elementary reaction". An elementary reaction, in turn, is definable as "a reaction for which no reaction intermediates have been detected or need to be postulated to describe a chemical reaction on a molecular scale" (both definitions are taken from [209]). Apparently, this definition can be hardly applied to the ubiquinol oxidation by bc_1. Under conditions where the heme b_1 is kept reduced (either by antimycin or by the backpressure from the membrane potential), the $Q_P^{\bullet-}$ semiquinone, although EPR-silent, is detectable as a reaction intermediate via its ability to reduce oxygen to superoxide. The formation of the latter can be monitored by EPR probes (see [210] and references therein), by fluorescent dyes [151], as well as via H_2O_2 formation (see [165] and references therein).

Trumpower has argued that "semiquinone at center P only exists as an aberrant by-product" and that the reduction of oxygen to superoxide by semiquinone "reflects the "error rate" at which the concerted reaction is disrupted" [207]. Kramer et al., however, have recently reported a similar pattern of thermal activation, including a unusual $E_a(H) > E_a(D)$ feature, for biomimetic systems, where the reaction of ubiquinol oxidation proceeds in two steps, and for the intact yeast bc_1 [208]. Based on these data, it was suggested that even in a non-inhibited bc_1 the oxidation of ubiquinol proceeds via two one-electron steps.

4.6. Logical gating/double gating

The idea of logical/double gating has been recently put forward by several authors to explain both the obligatory bifurcation of electron flows and the prevention of short circuits in bc_1 [20,88]. According to this view, a "productive" binding of ubiquinol in center P is possible only when all the potential electron and proton acceptors are, respectively, oxidized and deprotonated. And other way around, a productive ubiquinone binding is only possible when these electron and proton acceptors are reduced and protonated. This scheme provides an elegant explanation of the emptiness of catalytic center P in the crystal structures of bc_1: none of these "productive" states can be achieved at equilibrium. The here suggested scheme of ubiquinol oxidation (see Section 2.5 and Fig. 7) is compatible with the logical/double gating principle but, in addition, requires that the potential proton donors/acceptors, and especially the Glu-272 residue, have to be in the appropriate conformations. The difference between the here suggested scheme and the logical/double gating

becomes clear upon consideration of experimental data. For example, two following experimental observations can be rationalized in the framework of both schemes, although the consideration of the conformational mobility of Glu-272 provides a more elaborated picture.

(1) At steady state, bc_1 stops to oxidize ubiquinol in the presence of antimycin after both cytochrome b hemes become reduced, even if an oxidant, which keeps both the FeS cluster and cytochrome c_1 oxidized, is available [73].

(2) At high membrane potential, the cytochrome b becomes over-reduced while cytochrome c_1 stays oxidized. This situation, however, does not lead to the short-circuiting of bc_1 by the transfer of both electrons from the ubiquinol to the high-potential ET branch [200,201].

Although both observations are widely cited in evidence of an obligatory electron bifurcation in center P, the underlying mechanisms has remained unclear. In the framework of the logical/double gating, the reduced state of heme b_1 is expected to prevent a "productive" ubiquinol binding. On a more detailed level, the observations can be rationalized by a suggestion that the reduction of cytochrome b leads to the protonation of Glu-272 and to the trapping of its side chain in the "heme b_1" position (state C in Fig. 10) due to electrostatic and, perhaps, allosteric interactions, as discussed above. Then, as long as cytochrome b is reduced, Glu-272 is "turned away" and impeded in the formation of a hydrogen bond with the quinol ring. Thus, the ubiquinol oxidation is blocked already on the step of ubiquinol binding/first deprotonation. The turnover of bc_1 under such conditions is expected to resemble one in the Glu-272 → Gln mutant. And indeed, the residual activity of about 2%, which seems to be typical for an antimycin-inhibited bc_1 and which manifests itself both in the slow cytochrome c reduction [73] and in the generation of superoxide [164], is compatible to the residual activity of the corresponding Glu-295 → Gln mutant of *Rb. sphaeroides* [72].

The next experimental observation can be hardly explained by a logical/double gating alone, but requires the consideration of the conformational gating/Glu-272 switch:

(3) In the presence of antimycin, the flash-reduced hemes of cytochrome b remain reduced in the dark for seconds [85].

Because under these conditions, the FeS cluster is reduced by redox mediators at milliseconds, the logical/double gating mechanism would predict ubiquinone binding in center P followed by a thermodynamically favorable oxidation of cytochrome b. The absence of such oxidation can be rationalized by taking into account the role of Glu-272 in the semiquinone stabilization, which is crucial for reversed reactions in center P. The redox potential of ubisemiquinone is low in solutes with small ϵ_{eff}, on the order of -600 mV [211]. Therefore, a quinone in center P can be reduced only if the redox potential of the $Q_P/Q_P^{\bullet-}$ redox couple is elevated, due to the relative stabilization of the semiquinone by the

surrounding charged/polar groups, to acceptably high values. For example, as already noted in Section 2.4, the stabilization of the $Q_B^{\bullet-}$ semiquinone in the RC is accomplished, besides the electrostatic interaction with the iron atom [131], by a direct interaction with several amino acid residues [24]. It has been argued recently that specifically the formation of a hydrogen bond with Ser-L223 makes the reduction of Q_B by $Q_A^{\bullet-}$ possible [212]. When both hemes of cytochrome b are pre-reduced by flashes in the presence of antimycin, the participation of the Glu-272 in semiquinone stabilization is impeded by its trapping in the $Glu272_{bl}$ state in response to the electrostatic and, perhaps, allosteric impact from the reduced heme b_1 (i.e., the C $\leftrightarrow$ D equilibrium in Fig. 10 is strongly shifted to the left). The poor semiquinone stabilization would prevent the oxidation of the cytochrome b hemes via center P. The stability of the $Q_P^{\bullet-}$ semiquinone could be, in addition, allosterically affected by antimycin in center N (see above); the latter point deserves further experimental investigation.

A compatibly tight trapping of the protonated $Glu-272_{bl}$ state is not expected under conditions of the reverse electron transfer in bc_1. In this case, antimycin is absent, heme b_1 is oxidized, and only heme b_h is partly reduced [86]. Under these conditions, Glu-272 can contribute to the stabilization of a semiquinone and enable the ubiquinone reduction in center P.

Acknowledgments

References

[1] E.A. Berry, M. Guergova-Kuras, L.S. Huang, A.R. Crofts, Structure and function of cytochrome bc complexes, Annu. Rev. Biochem. 69 (2000) 1005–1075.

[2] W.A. Cramer, G.M. Soriano, M. Ponomarev, D. Huang, H. Zhang, S.E. Martinez, J.L. Smith, Some new structural aspects and old controversies concerning the cytochrome b_6f complex of oxygenic photosynthesis, Annu. Rev. Plant Physiol. Plant Mol. Biol. 47 (1996) 477–508.

[3] W.A. Cramer, D.B. Knaff, Energy Transduction in Biological Membranes: A Textbook of Bioenergetics, Springer-Verlag, 1990.

[4] C.A. Yu, J.Z. Xia, A.M. Kachurin, L. Yu, D. Xia, H. Kim, J. Deisenhofer, Crystallization and preliminary structure of beef heart mitochondrial cytochrome-bc_1 complex, Biochim. Biophys. Acta 1275 (1996) 47–53.

[5] D. Xia, C.A. Yu, H. Kim, J.Z. Xia, A.M. Kachurin, L. Zhang, L. Yu, J. Deisenhofer, Crystal structure of the cytochrome bc_1 complex from bovine heart mitochondria, Science 277 (1997) 60–66.

[6] Z. Zhang, L. Huang, V.M. Shulmeister, Y.I. Chi, K.K. Kim, L.W. Hung, A.R. Crofts, E.A. Berry, S.H. Kim, Electron transfer by domain movement in cytochrome bc_1, Nature 392 (1998) 677–684.

[7] S. Iwata, J.W. Lee, K. Okada, J.K. Lee, M. Iwata, B. Rasmussen, T.A. Link, S. Ramaswamy, B.K. Jap, Complete structure of the 11-subunit bovine mitochondrial cytochrome bc_1 complex, Science 281 (1998) 64–71.

[8] H. Kim, D. Xia, C.A. Yu, J.Z. Xia, A.M. Kachurin, L. Zhang, L. Yu, J. Deisenhofer, Inhibitor binding changes domain mobility in the iron–sulfur protein of the mitochondrial bc_1 complex from bovine heart, Proc. Natl. Acad. Sci. U. S. A. 95 (1998) 8026–8033.

[9] C. Hunte, J. Koepke, C. Lange, T. Rossmanith, H. Michel, Structure at 2.3 Å resolution of the cytochrome bc_1 complex from the yeast *Saccharomyces cerevisiae* co-crystallized with an antibody Fv fragment, Structure Fold. Des. 8 (2000) 669–684.

[10] C. Lange, C. Hunte, Crystal structure of the yeast cytochrome bc_1 complex with its bound substrate cytochrome c, Proc. Natl. Acad. Sci. U. S. A. 99 (2002) 2800–2805.

[11] E.A. Berry, L.S. Huang, L.K. Saechao, N.G. Pon, M. Valkova-Valchanova, F. Daldal, X-ray structure of cytochrome bc_1: comparison with its mitochondrial and chloroplast counterparts, Photosynth. Res. 81 (2004) 251–275.

[12] K.H. Xiao, A. Chandrasekaran, L. Yu, C.A. Yu, Evidence for the intertwined dimer of the cytochrome bc_1 complex in solution, J. Biol. Chem. 276 (2001) 46125–46131.

[13] K.H. Leung, P.C. Hinkle, Reconstitution of ion transport and respiratory control in vesicles formed from reduced coenzyme Q-cytochrome c reductase and phospholipids, J. Biol. Chem. 250 (1975) 8467–8471.

[14] E.C. Hurt, N. Gabellini, Y. Shahak, W. Lockau, G. Hauska, Extra proton translocation and membrane potential generation—Universal properties of cytochrome cytochrome bc_1/b_6f complexes reconstituted into liposomes, Arch. Biochem. Biophys. 225 (1983) 879–885.

[15] P. Mitchell, Proton motive redox mechanism of the cytochrome $b–c_1$ complex in the respiratory chain: proton motive ubiquinone cycle, FEBS Lett. 56 (1975) 1–6.

[16] P. Mitchell, Possible molecular mechanisms of the protonmotive function of cytochrom systems, J. Theor. Biol. 62 (1976) 327–367.

[17] M.K. Wikstrom, J.A. Berden, Oxidoreduction of cytochrome b in the presence of antimycin, Biochim. Biophys. Acta 283 (1972) 403–420.

[18] O.A. Gopta, B.A. Feniouk, W. Junge, A.Y. Mulkidjanian, The cytochrome bc_1 complex of *Rhodobacter capsulatus*: ubiquinol oxidation in a dimeric Q-cycle? FEBS Lett. 431 (1998) 291–296.

[19] C. Hunte, H. Palsdottir, B.L. Trumpower, Protonmotive pathways and mechanisms in the cytochrome bc_1 complex, FEBS Lett. 545 (2003) 39–46.

[20] A. Osyczka, C.C. Moser, F. Daldal, P.L. Dutton, Reversible redox energy coupling in electron transfer chains, Nature 427 (2004) 607–612.

[21] H. Myllykallio, F. Drepper, P. Mathis, F. Daldal, Electron-transfer supercomplexes in photosynthesis and respiration, Trends Microbiol. 8 (2000) 493–494.

[22] A. Matsuno-Yagi, Y. Hatefi, Ubiquinol: cytochrome c oxidoreductase (complex III)—Effect of inhibitors on cytochrome b reduction in submitochondrial particles and the role of ubiquinone in complex III, J. Biol. Chem. 276 (2001) 19006–19011.

[23] C.R.D. Lancaster, H. Michel, The coupling of light-induced

electron transfer and proton uptake as derived from crystal structures of reaction centres from *Rhodopseudomonas viridis* modified at the binding site of the secondary quinone, Q$_B$, Structure 5 (1997) 1339–1359.

[24] M.H. Stowell, T.M. McPhillips, D.C. Rees, S.M. Soltis, E. Abresch, G. Feher, Light-induced structural changes in photosynthetic reaction center: implications for mechanism of electron-proton transfer, Science 276 (1997) 812–816.

[25] A.Y. Mulkidjanian, Conformationally controlled pK-switching in membrane proteins: one more mechanism specific to the enzyme catalysis? FEBS Lett. 463 (1999) 199–204.

[26] D.A. Cherepanov, S.I. Bibikov, M.V. Bibikova, D.A. Bloch, L.A. Drachev, O.A. Gopta, D. Oesterhelt, A.Y. Semenov, A.Y. Mulkidjanian, Reduction and protonation of the secondary quinone acceptor of *Rhodobacter sphaeroides* photosynthetic reaction center: kinetic model based on a comparison of wild-type chromatophores with mutants carrying Arg → Ile substitution at sites 207 and 217 in the L-subunit, Biochim. Biophys. Acta 1459 (2000) 10–34.

[27] A.Y. Mulkidjanian, M.A. Kozlova, D.A. Cherepanov, Ubiquinone reduction in the photosynthetic reaction center of *Rhodobacter sphaeroides*: Interplay between electron transfer, proton binding and the flips of quinone ring, Biochem. Soc. Trans. 33 (2005) 845–850.

[28] M.L. Paddock, G. Feher, M.Y. Okamura, Proton transfer pathways and mechanism in bacterial reaction centers, FEBS Lett. 555 (2003) 45–50.

[29] C.A. Wraight, Proton and electron transfer in the acceptor quinone complex of photosynthetic reaction center from *Rhodobacter sphaeroides*, Front. Biosci. 9 (2004) 309–327.

[30] C. Hunte, Insights from the structure of the yeast cytochrome bc_1 complex: crystallization of membrane proteins with antibody fragments, FEBS Lett. 504 (2001) 126–132.

[31] X. Gao, X. Wen, L. Esser, B. Quinn, L. Yu, C.A. Yu, D. Xia, Structural basis for the quinone reduction in the bc_1 complex: a comparative analysis of crystal structures of mitochondrial cytochrome bc_1 with bound substrate and inhibitors at the Q$_i$ site, Biochemistry 42 (2003) 9067–9080.

[32] A.R. Crofts, The cytochrome bc_1 complex: function in the context of structure, Annu. Rev. Physiol. 66 (2004) 689–733.

[33] A.R. Crofts, C.A. Wraight, The electrochemical domain of photosynthesis, Biochim. Biophys. Acta 726 (1983) 149–185.

[34] J.B. Jackson, Bacterial photosynthesis, in: C. Anthony (Ed.), Bacterial energy transduction, Academic Press, London, 1988, pp. 317–376.

[35] R.B. Gennis, B. Barquera, B. Hacker, S.R. Van Doren, S. Arnaud, A.R. Crofts, E. Davidson, K.A. Gray, F. Daldal, The bc_1 complexes of *Rhodobacter sphaeroides* and *Rhodobacter capsulatus*, J. Bioenerg. Biomembr. 25 (1993) 195–209.

[36] P.L. Dutton, R.C. Prince, Reaction center-driven cytochrome interactions in electron and proton translocation and energy coupling, in: R.K. Clayton, W.R. Sistrom (Eds.), The Photosynthetic Bacteria, Plenum Press, New York, 1978, pp. 525–571.

[37] J.R. Bowyer, S.W. Meinhardt, G.V. Tierney, A.R. Crofts, Resolved difference spectra of redox centers involved in photosynthetic electron flow in *Rhodopseudomonas capsulata* and *Rhodopseudomonas sphaeroides*, Biochim. Biophys. Acta 635 (1981) 167–186.

[38] J.B. Jackson, A.R. Crofts, The kinetics of light induced carotenoid changes in *Rhodopseudomonas sphaeroides* and their relation to electrical field generation across the chromatophore membrane, Eur. J. Biochem. 18 (1971) 120–130.

[39] L.A. Drachev, M.D. Mamedov, A.Y. Mulkidjanian, A.Y. Semenov, V.P. Shinkarev, M.I. Verkhovsky, B.S. Kaurov, V.P. Skulachev, Flash-induced electrogenic events in the photosynthetic reaction center and cytochrome bc_1-complex of *Rhodobacter sphaeroides* chromatophores, Biochim. Biophys. Acta 973 (1989) 189–197.

[40] A.Y. Mulkidjanian, M.D. Mamedov, A.Y. Semenov, V.P. Shinkarev, M.I. Verkhovsky, L.A. Drachev, Partial reversion of electrogenic reaction in ubiquinol: cytochrome c_2 reductase of *Rhodobacter*

sphaeroides under the neutral and alkaline conditions, FEBS Lett. 277 (1990) 127–130.

[41] C.A. Wraight, R.J. Cogdell, B. Chance, Ion transport and electrochemical gradients in photosynthetic bacteria, in: R.K. Clayton, W.R. Sistrom (Eds.), The Photosynthetic Bacteria, Plenum Press, New York, 1978, pp. 471–511.

[42] K. Petty, J.B. Jackson, P.L. Dutton, Factors controlling the binding of two protons per electron transferred through the ubiquinone and cytochrome b/c_2 segment of *Rhodopseudomonas sphaeroides* chromatophores, Biochim. Biophys. Acta 546 (1979) 17–42.

[43] A.Y. Mulkidjanian, W. Junge, Calibration and time resolution of lumenal pH-transients in chromatophores of *Rhodobacter capsulatus* following a single turnover flash of light: proton release by the cytochrome bc_1-complex is strongly electrogenic, FEBS Lett. 353 (1994) 189–193.

[44] L. Yu, Q.C. Mei, C.A. Yu, Characterization of purified cytochrome $b–c_1$ complex from *Rhodopseudomonas sphaeroides* R-26, J. Biol. Chem. 259 (1984) 5752–5760.

[45] D.E. Robertson, H. Ding, P.R. Chelminski, C. Slaughter, J. Hsu, C. Moomaw, M. Tokito, F. Daldal, P.L. Dutton, Hydroubiquinonecytochrome c_2 oxidoreductase from *Rhodobacter capsulatus*: definition of a minimal, functional isolated preparation, Biochemistry 32 (1993) 1310–1317.

[46] G. Brasseur, A.S. Saribas, F. Daldal, A compilation of mutations located in the cytochrome b subunit of the bacterial and mitochondrial bc_1 complex, Biochim. Biophys. Acta 1275 (1996) 61–69.

[47] S.G.E. Andersson, A. Zomorodipour, J.O. Andersson, T. SicheritzPonten, U.C.M. Alsmark, R.M. Podowski, A.K. Naslund, A.S. Eriksson, H.H. Winkler, C.G. Kurland, The genome sequence of *Rickettsia prowazekii* and the origin of mitochondria, Nature 396 (1998) 133–140.

[48] J.R. Bowyer, A.R. Crofts, On the mechanism of photosynthetic electron transfer in *Rhodopseudomonas capsulata* and *Rhodopseudomonas sphaeroides*, Biochim. Biophys. Acta 636 (1981) 218–233.

[49] D.P. O'Keefe, P.L. Dutton, Cytochrome b oxidation and reduction reactions in the ubiquinone-cytochrome b/c_2 oxidoreductase from *Rhodopseudomonas sphaeroides*, Biochim. Biophys. Acta 635 (1981) 149–166.

[50] K. Matsuura, D.P. O'Keefe, P.L. Dutton, A reevaluation of the events leading to the electrogenic reaction and proton translocation in the ubiquinol-cytochrome c oxidoreductase of *Rhodopseudomonas sphaeroides*, Biochim. Biophys. Acta 722 (1983) 12–22.

[51] A.Y. Mulkidjanian, W. Junge, Electrogenic proton displacements in the cytochrome bc_1 complex of *Rhodobacter capsulatus*, in: P. Mathis (Ed.), Photosynthesis: From Light to Biosphere, vol. II, Kluwer Academic Publishers, Dordrecht, 1995, pp. 547–550.

[52] A.R. Crofts, S.W. Meinhardt, K.R. Jones, M. Snozzi, The role of the quinone pool in the cyclic electron transfer chain of *Rhodopseudomonas sphaeroides*, Biochim. Biophys. Acta 723 (1983) 202–218.

[53] O.A. Gopta, A.Y. Mulkidjanian, The cytochrome bc_1-complex of *Rhodobacter capsulatus*: does the reaction in the presence of antimycin A correspond to a single turnover of an untreated enzyme? in: G. Garab (Ed.), Photosynthesis: Mechanisms and Effects, Kluwer Academic Publishers, Dordrecht, 1998, pp. 1533–1536.

[54] S.S. Klishin, W. Junge, A.Y. Mulkidjanian, Flash-induced turnover of the cytochrome bc_1 complex in chromatophores of *Rhodobacter capsulatus*: binding of Zn^{2+} decelerates likewise the oxidation of cytochrome b, the reduction of cytochrome c_1 and the voltage generation, Biochim. Biophys. Acta 1553 (2002) 177–182.

[55] K.I. Takamiya, P.L. Dutton, Ubiquinone in *Rhodopseudomonas sphaeroides*. Some thermodynamic properties, Biochim. Biophys. Acta 546 (1979) 1–16.

[56] S. Meinhardt, A.R. Crofts, Kinetic and thermodynamic resolution of cytochrome c$_1$ and cytochrome c_2 from *Rhodopseudomonas sphaeroides*, FEBS Lett. 149 (1982) 223–227.

[57] V.P. Skulachev, V.V. Chistyakov, A.A. Jasaitis, E.G. Smirnova,

Inhibition of the respiratory chain by zinc ions, Biochem. Biophys. Res. Commun. 26 (1967) 1–6.

[58] T.A. Link, G. von Jagow, Zinc ions inhibit the Q_P center of bovine heart mitochondrial *cytochrome bc_1 complex* by blocking a protonatable group, J. Biol. Chem. 270 (1995) 25001–25006.

[59] S.S. Klishin, A.Y. Mulkidjanian, Proton transfer paths at the quinone oxidizing site of the *Rb. capsulatus* cytochrome *bc* complex, in: A. van der Est, D. Bruce (Eds.), Photosynthesis: Fundamental Aspects to Global Perspectives, Montreal, vol. 1, 2005, pp. 260–262.

[60] D.A. Cherepanov, A.Y. Mulkidjanian, Effect of dielectric relaxation on the kinetics of electron transfer in photosynthetic reaction centers, in: G. Garab (Ed.), Photosynthesis: Mechanisms and Effects, Kluwer Academic Publishers, Dordrecht, 1998, pp. 795–798.

[61] D.A. Cherepanov, L.I. Krishtalik, A.Y. Mulkidjanian, Photosynthetic electron transfer controlled by protein relaxation: analysis by Langevin stochastic approach, Biophys. J. 80 (2001) 1033–1049.

[62] C.C. Moser, J.M. Keske, K. Warncke, R.S. Farid, P.L. Dutton, Nature of biological electron transfer, Nature 355 (1992) 796–802.

[63] V.P. Shinkarev, A.R. Crofts, C.A. Wraight, The electric field generated by photosynthetic reaction center induces rapid reversed electron transfer in the bc_1 complex, Biochemistry 40 (2001) 12584–12590.

[64] A.Y. Mulkidjanian, M.D. Mamedov, L.A. Drachev, Slow electrogenic events in the cytochrome bc_1-complex of *Rhodobacter sphaeroides*: the electron transfer between cytochrome *b* hemes can be non-electrogenic, FEBS Lett. 284 (1991) 227–231.

[65] J. Zhu, T. Egawa, S.-R. Yeh, L. Yu, C.-A. Yu, Fast kinetic studies of mitochondrial cytochrome bc_1 complex, Biophys. J. 88 (2005) 326a.

[66] K.M. Petty, P.L. Dutton, Ubiquinone-cytochrome *b* electron and proton transfer: a functional pK on cytochrome b_{50} in *Rhodopseudomonas sphaeroides* membranes, Arch. Biochem. Biophys. 172 (1976) 346–353.

[67] F. Baymann, D.E. Robertson, P.L. Dutton, W. Mantele, Electrochemical and spectroscopic investigations of the cytochrome bc_1 complex from *Rhodobacter capsulatus*, Biochemistry 38 (1999) 13188–13199.

[68] S. Izrailev, A.R. Crofts, E.A. Berry, K. Schulten, Steered molecular dynamics simulation of the Rieske subunit motion in the cytochrome bc_1 complex, Biophys. J. 77 (1999) 1753–1768.

[69] S.J. Hong, N. Ugulava, M. Guergova-Kuras, A.R. Crofts, The energy landscape for ubihydroquinone oxidation at the Q_O site of the bc_1 complex in *Rhodobacter sphaeroides*, J. Biol. Chem. 274 (1999) 33931–33944.

[70] C.R.D. Lancaster, H. Michel, Three-dimensional structures of photosynthetic reaction centers, Photosynth. Res. 48 (1996) 65–74.

[71] E.A. Berry, Z. Zhang, H.D. Bellamy, L. Huang, Crystallographic location of two Zn^{2+}-binding sites in the avian cytochrome bc_1 complex, Biochim. Biophys. Acta 1459 (2000) 440–448.

[72] A.R. Crofts, S. Hong, N. Ugulava, B. Barquera, R. Gennis, M. Guergova-Kuras, E.A. Berry, Pathways for proton release during ubihydroquinone oxidation by the bc_1 complex, Proc. Natl. Acad. Sci. U. S. A. 96 (1999) 10021–10026.

[73] E.C. Slater, The mechanism of action of the respiratory inhibitor, antimycin, Biochim. Biophys. Acta 301 (1973) 129–154.

[74] E.G. Glaser, A.R. Crofts, A new electrogenic step in the ubiquinol: cytochrome c_2 oxidoreductase complex of *Rhodopseudomonas sphaeroides*, Biochim. Biophys. Acta 766 (1984) 322–333.

[75] D.E. Robertson, P.L. Dutton, The nature and magnitude of the charge-separation reactions of ubiquinol cytochrome c_2 oxidoreductase, Biochim. Biophys. Acta 935 (1988) 273–291.

[76] V.P. Shinkarev, A.L. Drachev, M.D. Mamedov, A.Y. Mulkidjanian, A.Y. Semenov, M.I. Verkhovsky, Light-induced electron transfer and electrogenic reactions in the bc_1-complex of photosynthetic purple bacterium *Rhodobacter sphaeroides*, in: G. Drews, E.A. Dawes (Eds.), Molecular Biology of Membrane-Bound Complexes in Phototrophic Bacteria, Plenum Press, New York, 1990, pp. 393–400.

[77] J.W. Cooley, F. Daldal, Spectroscopic observation of structurally

mediated cross-talk between the quinone reduction and hydroquinone oxidation sites of the cytochrome bc_1 complex, Biophys. J. 88 (2005) 326a.

[78] U. Brandt, G. von Jagow, Analysis of inhibitor binding to the mitochondrial cytochrome *c* reductase by fluorescence quench titration. Evidence for a 'catalytic switch' at the Q_O center, Eur. J. Biochem. 195 (1991) 163–170.

[79] U. Brandt, U. Haase, H. Schagger, G. von Jagow, Significance of the "Rieske" iron-sulfur protein for formation and function of the ubiquinol-oxidation pocket of mitochondrial cytochrome *c* reductase (bc_1 complex), J. Biol. Chem. 266 (1991) 19958–19964.

[80] A.R. Crofts, B. Barquera, R.B. Gennis, R. Kuras, M. Guergova-Kuras, E.A. Berry, Mechanism of ubiquinol oxidation by the bc_1 complex: different domains of the quinol binding pocket and their role in the mechanism and binding of inhibitors, Biochemistry 38 (1999) 15807–15826.

[81] L. Zhang, Z. Li, B. Quinn, L. Yu, C.A. Yu, Nonoxidizable ubiquinol derivatives that are suitable for the study of the ubiquinol oxidation site in the cytochrome bc_1 complex, Biochim. Biophys. Acta 1556 (2002) 226–232.

[82] H. Palsdottir, C.G. Lojero, B.L. Trumpower, C. Hunte, Structure of the yeast cytochrome bc_1 complex with a hydroxyquinone anion Q_O site inhibitor bound, J. Biol. Chem. 278 (2003) 31303–31311.

[83] L. Esser, B. Quinn, Y.F. Li, M. Zhang, M. Elberry, L. Yu, C.A. Yu, D. Xia, Crystallographic studies of quinol oxidation site inhibitors: a modified classification of inhibitors for the cytochrome bc_1 complex, J. Mol. Biol. 341 (2004) 281–302.

[84] X.G. Gao, X.L. Wen, C.A. Yu, L. Esser, S. Tsao, B. Quinn, L. Zhang, L. Yu, D. Xia, The crystal structure of mitochondrial cytochrome bc_1 in complex with famoxadone: the role of aromatic–aromatic interaction in inhibition, Biochemistry 41 (2002) 11692–11702.

[85] S. Meinhardt, A.R. Crofts, The role of cytochrome *b*-566 in the electron-transfer chain of *Rhodopseudomonas sphaeroides*, Biochim. Biophys. Acta 723 (1983) 219–230.

[86] T. Miki, M. Miki, Y. Orii, Membrane potential-linked reversed electron transfer in the beef hearth cytochrome bc_1 complex reconstituted into potassium-loaded phospholipid vesicles, J. Biol. Chem. 269 (1994) 1827–1833.

[87] F.L. Muller, A.G. Roberts, M.K. Bowman, D.M. Kramer, Architecture of the Q_O site of the cytochrome bc_1 complex probed by superoxide production, Biochemistry 42 (2003) 6493–6499.

[88] P.R. Rich, The quinone chemistry of *bc* complexes, Biochim. Biophys. Acta 1658 (2004) 165–171.

[89] U. Brandt, The chemistry and mechanics of ubihydroquinone oxidation at center *P* (Q_O) of the cytochrome bc_1 complex, Biochim. Biophys. Acta 1365 (1998) 261–268.

[90] A.R. Crofts, S. Hong, Z. Zhang, E.A. Berry, Physicochemical aspects of the movement of the Rieske iron sulfur protein during quinol oxidation by the bc_1 complex from mitochondria and photosynthetic bacteria, Biochemistry 38 (1999) 15827–15839.

[91] E. Darrouzet, F. Daldal, Movement of the iron–sulfur subunit beyond the *ef* loop of cytochrome *b* is required for multiple turnovers of the bc_1 complex but not for single turnover Q_O site catalysis, J. Biol. Chem. 277 (2002) 3471–3476.

[92] T.A. Link, The role of the 'Rieske' iron sulfur protein in the hydroquinone oxidation (Q_P) site of the cytochrome bc_1 complex. The 'proton-gated affinity change' mechanism, FEBS Lett. 412 (1997) 257–264.

[93] S.S. Klishin, A.Y. Mulkidjanian, Electron/proton coupling in the cytochrome bc_1 complex of *Rhodobacter capsulatus*, Biophys. J. 88 (2005) 326a.

[94] G. von Jagow, T. Ohnishi, The chromone inhibitor stigmatellin— Binding to the ubiquinol oxidation center at the C-side of the mitochondrial membrane, FEBS Lett. 185 (1985) 311–315.

[95] T.E. King, C.A. Yu, L. Yu, Y.L. Chiang, An examination of the components, sequence, mechanisms and their incertainities involved

in mitochondrial electron transport from succinate to cytochrome *c*, in: E. Quagliariello, S. Papa, F. Palmieri, E.C. Slater, N. Siliprandi (Eds.), Electron Transfer Chain and Oxidative Phosphorylation, North-Holland Publ Co., Amsterdam, 1975, pp. 105–118.

[96] C.H. Snyder, B.L. Trumpower, Ubiquinone at center N is responsible for triphasic reduction of cytochrome *b* in the cytochrome *bc*₁ complex, J. Biol. Chem. 274 (1999) 31209–31216.

[97] K.C. Hansen, B.E. Schultz, G. Wang, S.I. Chan, Reaction of *Escherichia coli* cytochrome *bo*₃ and mitochondrial cytochrome *bc*₁ with a photoreleasable decylubiquinol, Biochim. Biophys. Acta 1456 (2000) 121–137.

[98] H. Tian, L. Yu, M.W. Mather, C.A. Yu, Flexibility of the neck region of the Rieske iron–sulfur protein is functionally important in the cytochrome *bc*₁ complex, J. Biol. Chem. 273 (1998) 27953–27959.

[99] H. Tian, S. White, L. Yu, C.A. Yu, Evidence for the head domain movement of the Rieske iron–sulfur protein in electron transfer reaction of the cytochrome *bc*₁ complex, J. Biol. Chem. 274 (1999) 7146–7152.

[100] E. Darrouzet, M. Valkova-Valchanova, F. Daldal, Probing the role of the Fe–S subunit hinge region during Q_O site catalysis in *Rhodobacter capsulatus bc*₁ complex, Biochemistry 39 (2000) 15475–15483.

[101] M. Valkova-Valchanova, E. Darrouzet, C.R. Moomaw, C.A. Slaughter, F. Daldal, Proteolytic cleavage of the Fe–S subunit hinge region of *Rhodobacter capsulatus bc*₁ complex: effects of inhibitors and mutations, Biochemistry 39 (2000) 15484–15492.

[102] E. Darrouzet, M. Valkova-Valchanova, C.C. Moser, P.L. Dutton, F. Daldal, Uncovering the [2Fe2S] domain movement in cytochrome *bc*₁ and its implications for energy conversion, Proc. Natl. Acad. Sci. U. S. A. 97 (2000) 4567–4572.

[103] M. Brugna, S. Rodgers, A. Schricker, G. Montoya, M. Kazmeier, W. Nitschke, I. Sinning, A spectroscopic method for observing the domain movement of the Rieske iron–sulfur protein, Proc. Natl. Acad. Sci. U. S. A. 97 (2000) 2069–2074.

[104] E. Darrouzet, C.C. Moser, P.L. Dutton, F. Daldal, Large scale domain movement in cytochrome *bc*₁: a new device for electron transfer in proteins, Trends Biochem. Sci. 26 (2001) 445–451.

[105] A.G. Roberts, M.K. Bowman, D.M. Kramer, Certain metal ions are inhibitors of cytochrome *b*₆*f* complex 'Rieske' iron–sulfur protein domain movements, Biochemistry 41 (2002) 4070–4079.

[106] V.P. Shinkarev, D.R.J. Kolling, T.J. Miller, A.R. Crofts, Modulation of the midpoint potential of the [2Fe–2S] Rieske iron sulfur center by Q_O occupants in the *bc*₁ complex, Biochemistry 41 (2002) 14372–14382.

[107] J.W. Cooley, A.G. Roberts, M.K. Bowman, D.M. Kramer, F. Daldal, The raised midpoint potential of the [2Fe2S] cluster of cytochrome *bc*₁ is mediated by both the Q_O site occupants and the head domain position of the Fe–S protein subunit, Biochemistry 43 (2004) 2217–2227.

[108] J.W. Cooley, F. Daldal, Blockage of *bc*₁ complex turnover at the high potential *b* heme (*b*_h) or quinone reduction (Q_i) sites causes a decrease in [2Fe2S]–quinone interaction in *Rhodobacter capsulatus* membranes, Biophys. J. 86 (2004) 337A.

[109] E. Darrouzet, M. Valkova-Valchanova, F. Daldal, The [2Fe–2S] cluster *E*_m as an indicator of the iron–sulfur subunit position in the ubihydroquinone oxidation site of the cytochrome *bc*₁ complex, J. Biol. Chem. 277 (2002) 3464–3470.

[110] A.R. Crofts, M. Guergova-Kuras, R. Kuras, N. Ugulava, J.Y. Li, S.J. Hong, Proton-coupled electron transfer at the Q_O site: what type of mechanism can account for the high activation barrier? Biochim. Biophys. Acta 1459 (2000) 456–466.

[111] A.R. Crofts, V.P. Shinkarev, S.A. Dikanov, R.I. Samoilova, D. Kolling, Interactions of quinone with the iron–sulfur protein of the *bc*₁ complex: is the mechanism spring-loaded? Biochim. Biophys. Acta 1555 (2002) 48–53.

[112] A.Y. Mulkidjanian, V.P. Shinkarev, M.I. Verkhovsky, B.S. Kaurov, A

study of kinetic properties of the stable semiquinone of the reaction center secondary acceptor in chromatophores of nonsulfur purple bacteria, Biochim. Biophys. Acta 849 (1986) 150–161.

[113] O.A. Gopta, D.A. Bloch, D.A. Cherepanov, A.Y. Mulkidjanian, Temperature dependence of the electrogenic reaction in the Q_B site of the *Rhodobacter sphaeroides* photosynthetic reaction center: the Q_A⁻Q_B → Q_AQ_B⁻ transition, FEBS Lett. 412 (1997) 490–494.

[114] M.S. Graige, M.L. Paddock, J.M. Bruce, G. Feher, M.Y. Okamura, Mechanism of proton-coupled electron transfer for quinone (Q_B) reduction in reaction centers of *Rb. sphaeroides*, J. Am. Chem. Soc. 118 (1996) 9005–9016.

[115] O.A. Gopta, D.A. Cherepanov, A.Y. Semenov, A.Y. Mulkidjanian, D.A. Bloch, Effect of temperature and surface potential on the electrogenic proton uptake in the Q_B site of the *Rhodobacter sphaeroides* reaction center: Q_A^•⁻Q_B^•⁻ → Q_AQ_BH₂ transition, Photosynth. Res. 55 (1998) 309–316.

[116] J. Breton, Absence of large-scale displacement of quinone Q_B in bacterial photosynthetic reaction centers, Biochemistry 43 (2004) 3318–3326.

[117] R. Brudler, H.J. de Groot, W.B. van Liemt, P. Gast, A.J. Hoff, J. Lugtenburg, K. Gerwert, FTIR spectroscopy shows weak symmetric hydrogen bonding of the Q_B carbonyl groups in *Rhodobacter sphaeroides* R26 reaction centres, FEBS Lett. 370 (1995) 88–92.

[118] R. Hienerwadel, S. Grzybek, C. Fogel, W. Kreutz, M.Y. Okamura, M.L. Paddock, J. Breton, E. Nabedryk, W. Mantele, Protonation of Glu L212 following Q_B^•⁻ formation in the photosynthetic reaction center of *Rhodobacter sphaeroides*: evidence from time-resolved infrared spectroscopy, Biochemistry 34 (1995) 2832–2843.

[119] E. Nabedryk, J. Breton, R. Hienerwadel, C. Fogel, W. Mantele, M.L. Paddock, M.Y. Okamura, Fourier transforms infrared difference spectroscopy of secondary quinone acceptor photoreduction in proton transfer mutants of *Rhodobacter sphaeroides*, Biochemistry 34 (1995) 14722–14732.

[120] J. Breton, C. Boullais, G. Berger, C. Mioskowski, E. Nabedryk, Binding sites of quinones in photosynthetic bacterial reaction centers investigated by light-induced FTIR difference spectroscopy: symmetry of the carbonyl interactions and close equivalence of the Q_B vibrations in *Rhodobacter sphaeroides* and *Rhodobacter capsulatus* probed by isotope labeling, Biochemistry 34 (1995) 11606–11616.

[121] V.P. Shinkarev, K.N. Timofeev, D.A. Cherepanov, A.A. Kononenko, Effect of quinones on temperature relationship of electron-transfer in the reaction center of purple bacteria, Biofizika 32 (1987) 168–169.

[122] M.A. Kozlova, D.A. Cherepanov, L. Baciou, P. Sebban, A.Y. Mulkidjanian, Electron transfer coupled protein relaxation in reaction centers of *Rb. sphaeroides*, in: A. van der Est, D. Bruce (Eds.), Photosynthesis: Fundamental Aspects to Global Perspectives, Montreal, vol. 1, 2005, pp. 222–224.

[123] R. Hienerwadel, S. Grzybek, M. Paddock, M. Okamura, W. Mäntele, Temperature-dependence of time-resolved IR signals associated with electron and proton transfer upon Q_B reduction in reaction centers of *Rb. sphaeroides*, in: J. Breton, E. Nabedryk, A. Vermeglio (Eds.), Reaction Centers of Photosynthetic Purple Bacteria: Structure, Spectroscopy, Dynamics, CEA, Direction des Sciences du Vivant, Cadarache, France, 1997.

[124] N. Ginet, J. Lavergne, Equilibrium and kinetic parameters for the binding of inhibitors to the Q_B pocket in bacterial chromatophores: dependence on the state of Q_A, Biochemistry 40 (2001) 1812–1823.

[125] J.P. Allen, G. Feher, T.O. Yeates, H. Komiya, D.C. Rees, Structure of the reaction center from *Rhodobacter capsulatus* R-26: the cofactors, Proc. Natl. Acad. Sci. U. S. A. 84 (1987) 5730–5734.

[126] C.-H. Chang, El-Kabbani, D. Tiede, J. Norris, M. Schiffer, The structure of the membrane-bound protein photosynthetic reaction center from *Rhodobacter sphaeroides*, Biochemistry 30 (1991) 5352–5360.

[127] M.L. Paddock, S.H. Rongey, G. Feher, M.Y. Okamura, Pathway of

proton transfer in bacterial reaction centers: replacement of Glu 212 in the L subunit inhibits quinone (Q_B) turnover, Proc. Natl. Acad. Sci. U. S. A. 86 (1989) 6602–6606.

[128] A.K. Grafton, R.A. Wheeler, Amino acid protonation states determine binding sites of the secondary ubiquinone and its anion in the *Rhodobacter sphaeroides* photosynthetic reaction center, J. Phys. Chem. B 103 (1999) 5380–5387.

[129] S.E. Walden, R.A. Wheeler, Protein conformational gate controlling binding site preference and migration for ubiquinone-B in the photosynthetic reaction center of *Rhodobacter sphaeroides*, J. Phys. Chem. B 106 (2002) 3001–3006.

[130] H. Ishikita, G. Morra, E.W. Knapp, Redox potential of quinones in photosynthetic reaction centers from *Rhodobacter sphaeroides*: dependence on protonation of Glu-L212 and Asp-L213, Biochemistry 42 (2003) 3882–3892.

[131] M. Nonella, K. Schulten, Molecular-dynamics simulation of electron-transfer in proteins—Theory and application to $Q_A \rightarrow Q_B$ transfer in the photosynthetic reaction center, J. Phys. Chem. 95 (1991) 2059–2067.

[132] V.P. Shinkarev, C.A. Wraight, Electron and proton transfer in the acceptor quinone complex of reaction centers of phototrophic bacteria, in: J. Deisenhofer, J.R. Norris (Eds.), The Photosynthetic Reaction Center, vol. 1, Academic Press, San Diego, 1993, pp. 193–255.

[133] V.P. Shinkarev, E. Takahashi, C.A. Wraight, Flash-induced electric-potential generation in wild-type and L212EQ mutant chromatophores of *Rhodobacter-sphaeroides*—Q_BH_2 is not released from L212EQ mutant reaction centers, Biochim. Biophys. Acta 1142 (1993) 214–216.

[134] E. Takahashi, C.A. Wraight, Proton and electron transfer in the acceptor quinone complex of *Rhodobacter sphaeroides* reaction centers: characterization of site-directed mutants of the two ionizable residues, GluL212 and AspL213, in the Q_B binding site, Biochemistry 31 (1992) 855–866.

[135] U. Ermler, G. Fritzsch, S.K. Buchanan, H. Michel, Structure of the photosynthetic reaction center from *Rhodobacter sphaeroides* at 2.65 Å resolution: cofactors and protein–cofactor interactions, Structure 2 (1994) 925–936.

[136] E.A. Berry, L.S. Huang, Observations concerning the quinol oxidation site of the cytochrome bc_1 complex, FEBS Lett. 555 (2003) 13–20.

[137] T.A. Link, The structure of Rieske and Rieske-type proteins, Adv. Inorg. Chem. 47 (1999) 83–157.

[138] N.B. Ugulava, A.R. Crofts, CD-monitored redox titration of the Rieske Fe–S protein of *Rhodobacter sphaeroides*: pH dependence of the midpoint potential in isolated bc_1 complex and in membranes, FEBS Lett. 440 (1998) 409–413.

[139] R. Covian, R. Moreno-Sanchez, Role of protonatable groups of bovine heart bc_1 complex in ubiquinol binding and oxidation, Eur. J. Biochem. 268 (2001) 5783–5790.

[140] Y. Zu, M.M. Couture, D.R. Kolling, A.R. Crofts, L.D. Eltis, J.A. Fee, J. Hirst, Reduction potentials of Rieske clusters: importance of the coupling between oxidation state and histidine protonation state, Biochemistry 42 (2003) 12400–12408.

[141] P.R. Rich, Electron and proton transfers through quinones and cytochrome *bc* complexes, Biochim. Biophys. Acta 768 (1984) 53–79.

[142] P.H. McPherson, M.Y. Okamura, G. Feher, Electron transfer from the reaction center of *Rb. sphaeroides* to the quinone pool: doubly reduced Q_B leaves the reaction center, Biochim. Biophys. Acta 1016 (1990) 289–292.

[143] L.A. Drachev, M.D. Mamedov, A.Y. Mulkidjanian, A.Y. Semenov, V.P. Shinkarev, M.I. Verkhovsky, Electrogenesis associated with proton transfer in the reaction center protein of the purple bacterium *Rhodobacter sphaeroides*, FEBS Lett. 259 (1990) 324–326.

[144] P. Brzezinski, G. Larsson, Redox-driven proton pumping by heme-copper oxidases, Biochim. Biophys. Acta 1605 (2003) 1–13.

[145] S. Junemann, P. Heathcote, P.R. Rich, On the mechanism of quinol oxidation in the bc_1 complex, J. Biol. Chem. 273 (1998) 21603–21607.

[146] W.W. Parson, Quinones as secondary electron acceptors, in: R.K. Clayton, W.R. Sistrom (Eds.), The Photosynthetic Bacteria, Plenum Press, New York, 1978, pp. 455–469.

[147] C.A. Wraight, The role of quinones in bacterial photosynthesis, Photochem. Photobiol. 30 (1979) 767–776.

[148] A.W. Rutherford, M.C. Evans, Direct measurement of the redox potential of the primary and secondary quinone electron acceptors in *Rhodopseudomonas sphaeroides* (wild-type) by EPR spectrometry, FEBS Lett. 110 (1980) 257–261.

[149] V.D. Sled', A.Y. Mulkidjanian, V.P. Shinkarev, M.I. Verkhovsky, B.S. Kaurov, A.B. Rubin, Direct spectrophotometric determination of the midpoint potential of primary and secondary quinone acceptors of photosynthetic reaction center, Biokhimiya 49 (1984) 204–208.

[150] V.P. Shinkarev, A.Y. Mulkidjanian, M.I. Verkhovsky, B.S. Kaurov, Investigation of the kinetic and thermodynamic properties of the photosynthetic reaction center secondary acceptor in chromatophore membrane of nonsulphur purple bacteria, Biol. Membr. 2 (1985) 725–737.

[151] L. Zhang, L. Yu, C.A. Yu, Generation of superoxide anion by succinate-cytochrome *c* reductase from bovine heart mitochondria, J. Biol. Chem. 273 (1998) 33972–33976.

[152] V.A. Roginsky, L.M. Pisarenko, W. Bors, C. Michel, The kinetics and thermodynamics of quinone-semiquinone-hydroquinone systems under physiological conditions, J. Chem. Soc., Perkin Trans. 2 (1999) 871–876.

[153] P.R. Rich, D.S. Bendall, The kinetics and thermodynamics of the reduction of cytochrome *c* by substituted p-benzoquinols in solution, Biochim. Biophys. Acta 592 (1980) 506–518.

[154] P.R. Rich, D.S. Bendall, A mechanism for the reduction of cytochromes by quinols in solution and its relevance to biological electron transfer reactions, FEBS Lett. 105 (1979) 189–194.

[155] B.J. van Rotterdam, H.V. Westerhoff, R.W. Visschers, M.R. Jones, K.J. Hellingwerf, W. Crielaard, Steady-state cyclic electron transfer through solubilized *Rhodobacter sphaeroides* reaction centres, Biophys. Chem. 88 (2000) 137–152.

[156] A.R. Crofts, Proton-coupled electron transfer at the Q_O-site of the bc_1 complex controls the rate of ubihydroquinone oxidation, Biochim. Biophys. Acta 1655 (2004) 77–92.

[157] L.I. Krishtalik, pH-dependent redox potential: how to use it correctly in the activation energy analysis, Biochim. Biophys. Acta 1604 (2003) 13–21.

[158] S. Heimann, M.V. Ponamarev, W.A. Cramer, Movement of the Rieske iron-sulfur protein in the *p*-side bulk aqueous phase: effect of lumenal viscosity on redox reactions of the cytochrome $b_6 f$ complex, Biochemistry 39 (2000) 2692–2699.

[159] C.C. Page, C.C. Moser, X.X. Chen, P.L. Dutton, Natural engineering principles of electron tunnelling in biological oxidation–reduction, Nature 402 (1999) 47–52.

[160] H.B. Gray, J.R. Winkler, Electron transfer in proteins, Annu. Rev. Biochem. 65 (1996) 537–561.

[161] J.L. Li, D. Gilroy, D.M. Tiede, M.R. Gunner, Kinetic phases in the electron transfer from $P^+Q_A^{\bullet-}Q_B$ to $P^+Q_AQ_B^{\bullet-}$ and the associated processes in *Rhodobacter sphaeroides* R-26 reaction centers, Biochemistry 37 (1998) 2818–2829.

[162] C.A. Yu, X.L. Wen, K.H. Xiao, D. Xia, L. Yu, Inter- and intra-molecular electron transfer in the cytochrome bc_1 complex, Biochim. Biophys. Acta 1555 (2002) 65–70.

[163] M.I. Verkhovsky, J.E. Morgan, A. Puustein, M. Wikstrom, Kinetic trapping of oxygen in cell respiration, Nature 380 (1996) 268–270.

[164] F. Muller, A.R. Crofts, D.M. Kramer, Multiple Q-cycle bypass reactions at the Q_O site of the cytochrome bc_1 complex, Biochemistry 41 (2002) 7866–7874.

[165] D.M. Kramer, A.G. Roberts, F. Muller, J. Cape, M.K. Bowman,

Q-cycle bypass reactions at the Q_O site of the cytochrome bc_1 (and related) complexes, Methods Enzymol. 382 (2004) 21–45.

[166] M. Guergova-Kuras, R. Kuras, N. Ugulava, I. Hadad, A.R. Crofts, Specific mutagenesis of the Rieske iron–sulfur protein in *Rhodobacter sphaeroides* shows that both the thermodynamic gradient and the pK of the oxidized form determine the rate of quinol oxidation by the bc_1 complex, Biochemistry 39 (2000) 7436–7444.

[167] C.H. Snyder, E.B. Gutierrez-Cirlos, B.L. Trumpower, Evidence for a concerted mechanism of ubiquinol oxidation by the cytochrome bc_1 complex, J. Biol. Chem. 275 (2000) 13535–13541.

[168] R.A. Marcus, N. Sutin, Electron transfers in chemistry and biology, Biochim. Biophys. Acta 811 (1985) 265–322.

[169] C.R.D. Lancaster, Ubiquinone reduction and protonation in photosynthetic reaction centres from *Rhodopseudomonas viridis*: X-ray structures and their functional implications, Biochim. Biophys. Acta 1365 (1998) 143–150.

[170] S. de Vries, S.P. Albracht, J.A. Berden, E.C. Slater, The pathway of electrons through QH_2:cytochrome c oxidoreductase studied by pre-steady-state kinetics, Biochim. Biophys. Acta 681 (1982) 41–53.

[171] S. de Vries, S.P. Albracht, J.A. Berden, C.A. Marres, E.C. Slater, The effect of pH, ubiquinone depletion and myxothiazol on the reduction kinetics of the prosthetic groups of ubiquinol:cytochrome c oxidoreductase, Biochim. Biophys. Acta 723 (1983) 91–103.

[172] P. Mitchell, J. Moyle, The role of ubiquinone and plastoquinone in chemiosmotic coupling between electron transfer and proton translocation, in: G. Lenaz (Ed.), Coenzyme Q, John Willey and Sons Ltd., Chinester, 1985, pp. 145–165.

[173] X. Gong, L. Yu, D. Xia, C.A. Yu, Evidence for electron equilibrium between the two hemes b_1 in the dimeric cytochrome bc_1 complex, J. Biol. Chem. 280 (2005) 9251–9257.

[174] M.A. Selak, J. Whitmarsh, Kinetics of the electrogenic step and cytochrome b_6 and f redox changes in chloroplasts. Evidence for a Q cycle, FEBS Lett. 150 (1982) 286–292.

[175] P.R. Rich, P. Heathcote, D.A. Moss, Kinetic studies of electron transfer in a hybrid system constructed from the cytochrome bf complex and photosystem I, Biochim. Biophys. Acta 892 (1987) 138–151.

[176] D.P. O'Keefe, Structure and function of the chloroplast cytochrome bf complex, Photosynth. Res. 17 (1988) 189–216.

[177] A.B. Hope, R.R. Huilgol, M. Panizza, M. Thompson, D.B. Matthews, The flash-induced turnover of cytochrome-b-563, cytochrome-f and plastocyanin in chloroplasts—Models and estimation of kinetic-parameters, Biochim. Biophys. Acta 1100 (1992) 15–26.

[178] M.V. Ponamarev, W.A. Cramer, Perturbation of the internal water chain in cytochrome f of oxygenic photosynthesis: loss of the concerted reduction of cytochromes f and b_6, Biochemistry 37 (1998) 17199–17208.

[179] A.R. Crofts, V.P. Shinkarev, D.R. Kolling, S. Hong, The modified Q-cycle explains the apparent mismatch between the kinetics of reduction of cytochrome c_1 and b_h in the bc_1 complex, J. Biol. Chem. 278 (2003) 36191–36201.

[180] B.E. Schultz, S.I. Chan, Structures and proton-pumping strategies of mitochondrial respiratory enzymes, Annu. Rev. Biophys. Biomol. Struct. 30 (2001) 23–65.

[181] C.L. Colbert, M.M. Couture, L.D. Eltis, J.T. Bolin, A cluster exposed: structure of the Rieske ferredoxin from biphenyl dioxygenase and the redox properties of Rieske Fe–S proteins, Structure Fold. Des. 8 (2000) 1267–1278.

[182] J.R. Bowyer, P.L. Dutton, R.C. Prince, A.R. Crofts, The role of the Rieske iron-sulfur center as the electron donor to ferricytochrome c_2 in *Rhodopseudomonas sphaeroides*, Biochim. Biophys. Acta 592 (1980) 445–460.

[183] J.S. Rieske, Experimental observations on the structure and function of mitochondrial complex III that are unresolved by the protonmotive ubiquinone-cycle hypothesis, J. Bioenerg. Biomembr. 18 (1986) 235–257.

[184] N. Howell, D.E. Robertson, Electrochemical and spectral-analysis of the long-range interactions between the Q_O and Q_i sites and the heme prosthetic groups in ubiquinol cytochrome-c oxidoreductase, Biochemistry 32 (1993) 11162–11172.

[185] M. Iwaki, A. Osyczka, C.C. Moser, P.L. Dutton, P.R. Rich, ATR-FTIR spectroscopy studies of iron–sulfur protein and cytochrome c_1 in the *Rhodobacter capsulatus* cytochrome bc_1 complex, Biochemistry 43 (2004) 9477–9486.

[186] A. Warshel, S.T. Russell, Calculations of electrostatic interactions in biological systems and in solutions, Q. Rev. Biophys. 17 (1984) 283–422.

[187] A.Y. Mulkidjanian, D.A. Cherepanov, M. Haumann, W. Junge, Photosystem II of green plants: topology of core pigments and redox cofactors as inferred from electrochromic difference spectra, Biochemistry 35 (1996) 3093–3107.

[188] D.A. Cherepanov, A.Y. Mulkidjanian, Proton transfer in *Azotobacter vinelandii* ferredoxin: I. Entatic Lys84 operates as elastic counterbalance for the proton-carrying Asp15, Biochim. Biophys. Acta 1505 (2001) 179–184.

[189] K. Chen, J. Hirst, R. Camba, C.A. Bonagura, C.D. Stout, B.K. Burgess, F.A. Armstrong, Atomically defined mechanism for proton transfer to a buried redox centre in a protein, Nature 405 (2000) 814–817.

[190] G. Palmer, E.M. Degli, Application of exciton coupling theory to the structure of mitochondrial cytochrome b, Biochemistry 33 (1994) 176–185.

[191] A.J. Swallow, Physical chemistry of semiquinones, in: B.L. Trumpower (Ed.), Function of Quinones in Energy Conserving Systems, Academic Press, New York, 1982, pp. 59–72.

[192] C. Hagerhall, S. Magnitsky, V.D. Sled, I. Schroder, R.P. Gunsalus, G. Cecchini, T. Ohnishi, An *Escherichia coli* mutant quinol:fumarate reductase contains an EPR-detectable semiquinone stabilized at the proximal quinone-binding site, J. Biol. Chem. 274 (1999) 26157–26164.

[193] C.R.D. Lancaster, Quinone-binding sites in membrane proteins: what can we learn from the *Rhodobacter capsulatus* reaction centre? Biochem. Soc. Trans. 27 (1999) 591–596.

[194] H. Ding, D.E. Robertson, F. Daldal, P.L. Dutton, Cytochrome bc_1 complex [2Fe–2S] cluster and its interaction with ubiquinone and ubihydroquinone at the Q_O site: a double-occupancy Q_O site model, Biochemistry 31 (1992) 3144–3158.

[195] H. Ding, C.C. Moser, D.E. Robertson, M.K. Tokito, F. Daldal, P.L. Dutton, Ubiquinone pair in the Q_O site central to the primary energy conversion reactions of cytochrome bc_1 complex, Biochemistry 34 (1995) 15979–15996.

[196] A.G. Roberts, D.M. Kramer, Inhibitor "double occupancy" in the Q_O pocket of the chloroplast cytochrome b_6f complex, Biochemistry 40 (2001) 13407–13412.

[197] S. Bartoschek, M. Johansson, B.H. Geierstanger, J.G. Okun, C.R.D. Lancaster, E. Humpfer, L. Yu, C.A. Yu, C. Griesinger, U. Brandt, Three molecules of ubiquinone bind specifically to mitochondrial cytochrome bc_1 complex, J. Biol. Chem. 276 (2001) 35231–35234.

[198] U. Brandt, Bifurcated ubihydroquinone oxidation in the cytochrome bc_1 complex by proton-gated charge transfer, FEBS Lett. 387 (1996) 1–6.

[199] U. Brandt, J.G. Okun, Role of deprotonation events in ubihydroquinone:cytochrome c oxidoreductase from bovine heart and yeast mitochondria, Biochemistry 36 (1997) 11234–11240.

[200] M.K. Wikstrom, The different cytochrome b components in the respiratory chain of animal mitochondria and their role in electron transport and energy conservation, Biochim. Biophys. Acta 301 (1973) 155–193.

[201] M. Wikstrom, K. Krab, M. Saraste, Proton-translocating cytochrome complexes, Annu. Rev. Biochem. 50 (1981) 623–655.

[202] J.M. Mayer, I.J. Rhile, Thermodynamics and kinetics of proton-coupled electron transfer: stepwise vs. concerted pathways, Biochim. Biophys. Acta 1655 (2004) 51–58.

[203] J.M. Mayer, Proton-coupled electron transfer: a reaction chemist's view, Annu. Rev. Phys. Chem. 55 (2004) 363–390.

[204] C. Deniau, F. Rappaport, New insights on the proton pump associated with cytochrome $b_6 f$ turnovers from the study of H/D substitution effects on the electrogenicity and electron transfer reactions, Biochemistry 39 (2000) 3304–3310.

[205] R. Malkin, Redox properties of the DBMIB-Rieske iron sulfur complex in spinach chloroplast membranes, FEBS Lett. 131 (1981) 169–172.

[206] B. Schoepp, M. Brugna, A. Riedel, W. Nitschke, D.M. Kramer, The Q_O-site inhibitor DBMIB favours the proximal position of the chloroplast Rieske protein and induces a pK-shift of the redox-linked proton, FEBS Lett. 450 (1999) 245–250.

[207] B.L. Trumpower, A concerted, alternating sites mechanism of ubiquinol oxidation by the dimeric cytochrome bc_1 complex, Biochim. Biophys. Acta 1555 (2002) 166–173.

[208] D.M. Kramer, J.L. Cape, M.K. Bowman, Proton coupled electron transfer during hydroquinone oxidation in bc complexes and in a biomimetic system, in: A. van der Est, D. Bruce (Eds.), Photosynthesis: Fundamental Aspects to Global Perspectives, Montreal, in press.

[209] A.D. McNaught, A. Wilkinson, Compendium of Chemical Terminology, 2nd ed., Blackwell Science, 1997.

[210] M. Ksenzenko, A.A. Konstantinov, G.B. Khomutov, A.N. Tikhonov, E.K. Ruuge, Effect of electron-transfer inhibitors on superoxide generation in the cytochrome-bc_1 site of the mitochondrial respiratory chain, FEBS Lett. 155 (1983) 19–24.

[211] R.C. Prince, P.L. Dutton, J.M. Bruce, Electrochemistry of ubiquinones: menaquinones and plastoquinones in aprotic solvents, FEBS Lett. 160 (1983) 273–276.

[212] H. Ishikita, E.W. Knapp, Variation of Ser-L223 hydrogen bonding with the Q_B redox state in reaction centers from *Rhodobacter sphaeroides*, J. Am. Chem Soc. 126 (2004) 8059–8064.

[213] D.E. Robertson, E. Davidson, R.C. Prince, W.H. van den Berg, B.L. Marrs, P.L. Dutton, Discrete catalytic sites for quinone in the ubiquinol-cytochrome c_2 oxidoreductase of *Rhodopseudomonas capsulata*. Evidence from a mutant defective in ubiquinol oxidation, J. Biol. Chem. 261 (1986) 584–591.

[214] C.-H. Yun, A.R. Crofts, R.B. Gennis, Assignment of histidine axial ligands to the cytochrome b_h and cytochrome b_l components of the bc_1 complex from *Rhodobacter sphaeroides* site directed mutagenesis, Biochemistry 30 (1991) 6747–6754.

[215] E. Davidson, T. Ohnishi, E. Atta-Asafo-Adjei, F. Daldal, Potential ligands to the [2Fe–2S] Rieske cluster of the cytochrome bc_1 complex of *Rhodobacter capsulatus* probed by site-directed mutagenesis, Biochemistry 31 (1992) 3342–3351.

[216] W. Humphrey, A. Dalke, K. Schulten, VMD: visual molecular dynamics, J. Mol. Graphics 14 (1996) 33–38.

[217] D.A. Cherepanov, B.A. Feniouk, W. Junge, A.Y. Mulkidjanian, Low dielectric permittivity of water at the membrane interface: effect on the energy coupling mechanism in biological membranes, Biophys. J. 85 (2003) 1307–1316.

[218] D.A. Cherepanov, W. Junge, A.Y. Mulkidjanian, Proton transfer dynamics at the membrane/water interface: dependence on the fixed and mobile pH buffers, the geometry of membrane particles, and the interfacial potential barrier, Biophys. J. 86 (2004) 665–680.

[219] A.J. Chirino, E.J. Lous, M. Huber, J.P. Allen, C.C. Schenck, M.L. Paddock, G. Feher, D.C. Rees, Crystallographic analyses of site-directed mutants of the photosynthetic reaction center from *Rhodobacter sphaeroides*, Biochemistry 33 (1994) 4584–4593.

[220] H.L. Axelrod, E.C. Abresch, M.Y. Okamura, A.P. Yeh, D.C. Rees, G. Feher, X-ray structure determination of the cytochrome c_2: reaction center electron transfer complex from *Rhodobacter sphaeroides*, J. Mol. Biol. 319 (2002) 501–515.

[221] A.A. Konstantinov, Vectorial electron and proton transfer in the cytochrome bc_1 complexes, Biochim. Biophys. Acta 1018 (1990) 138–141.

[222] M. Iwaki, L. Giotta, A.O. Akinsiku, H. Schagger, N. Fisher, J. Breton, P.R. Rich, Redox-induced transitions in bovine cytochrome bc_1 complex studied by perfusion-induced ATR-FTIR spectroscopy, Biochemistry 42 (2003) 11109–11119.